AD-A165 295 A PHYSICAL MODEL AND CONSERVATION EQUATIONS FOR DYNAMIC 1/2
SOLID-LIQUID BEHAVIOR(U) VILLANOVA UNIV PA DEPT OF
MECHANICAL ENGINEERING J N MAJERUS FEB 86 BRL-CR-551

UNCLASSIFIED DAAK11-83-K-0009 F/G 20/4 NL

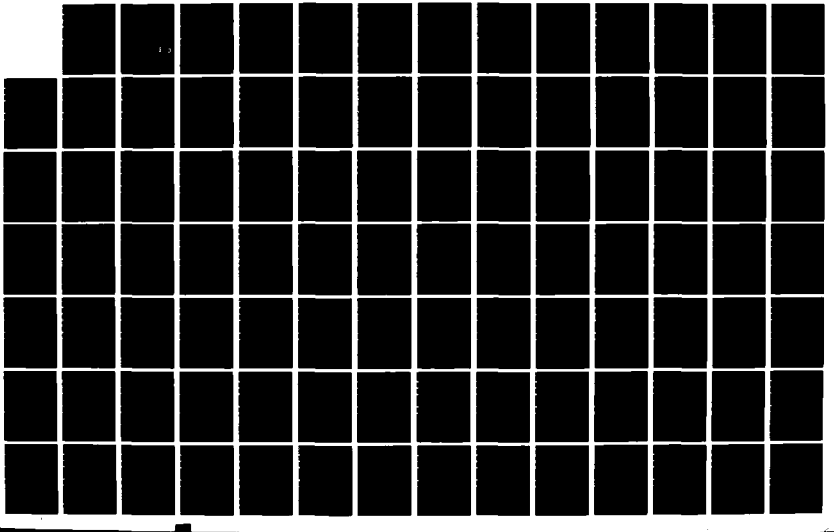

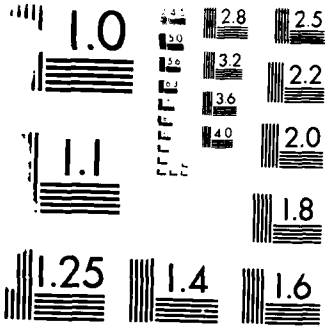

MICROCOPY RESOLUTION TEST CHART
NATIONAL BUREAU OF STANDARDS-1963-A

AD-A165 295

(12)

AD

US ARMY MATERIEL COMMAND

CONTRACT REPORT BRL-CR-551

A PHYSICAL MODEL AND CONSERVATION EQUATIONS FOR DYNAMIC SOLID-LIQUID BEHAVIOR

Mechanical Engineering Department
Villanova University
Villanova, PA 19085

February 1986

DTIC FILE COPY

DTIC ELECTE MAR 1 1 1986 S D D

APPROVED FOR PUBLIC RELEASE; DISTRIBUTION UNLIMITED.

US ARMY BALLISTIC RESEARCH LABORATORY
ABERDEEN PROVING GROUND, MARYLAND

86 3 11 064

Destroy this report when it is no longer needed.
Do not return it to the originator.

Additional copies of this report may be obtained from the National Technical Information Service, U. S. Department of Commerce, Springfield, Virginia 22161.

The findings in this report are not to be construed as an official Department of the Army position, unless so designated by other authorized documents.

The use of trade names or manufacturers' names in this report does not constitute indorsement of any commercial product.

Unclassified

SECURITY CLASSIFICATION OF THIS PAGE *(When Data Entered)*

REPORT DOCUMENTATION PAGE		READ INSTRUCTIONS BEFORE COMPLETING FORM
1. REPORT NUMBER Contract Report BRL-CR-551	2. GOVT ACCESSION NO. AD-A165295	3. RECIPIENT'S CATALOG NUMBER
4. TITLE *(and Subtitle)* A Physical Model and Conservation Equations for Dynamic Solid-Liquid Behavior		5. TYPE OF REPORT & PERIOD COVERED Progress, August 1983-April 1985. 6. PERFORMING ORG. REPORT NUMBER
7. AUTHOR(s) **John N. Majerus**		8. CONTRACT OR GRANT NUMBER(s) DAAK-11-83-K-0009
9. PERFORMING ORGANIZATION NAME AND ADDRESS Mechanical Engineering Department Villanova University Villanova, PA 19085		10. PROGRAM ELEMENT, PROJECT, TASK AREA & WORK UNIT NUMBERS
11. CONTROLLING OFFICE NAME AND ADDRESS US Army Ballistic Research Laboratory ATTN: **SLCBR-DD-T** Aberdeen Proving Ground, MD 21005-5066		12. REPORT DATE February 1986 13. NUMBER OF PAGES 114
14. MONITORING AGENCY NAME & ADDRESS*(if different from Controlling Office)*		15. SECURITY CLASS. *(of this report)* Unclassified 15a. DECLASSIFICATION DOWNGRADING SCHEDULE

16. DISTRIBUTION STATEMENT *(of this Report)*

Approved for Public Release; Distribution Unlimited.

17. DISTRIBUTION STATEMENT *(of the abstract entered in Block 20, if different from Report)*

18. SUPPLEMENTARY NOTES

19. KEY WORDS *(Continue on reverse side if necessary and identify by block number)*

Conservation equations
Constitutive equations
finite elements
fluid mechanics
nonlinear mechanics
numerical methods
penetration mechanics
solid mechanics
solution techniques
weighted residuals

20. ABSTRACT *(Continue on reverse side if necessary and identify by block number)*

A self-consistent set of equations were developed for 3-D penetration problems. The set of equations includes polymorphic and thermodynamic phase changes, finite material extensions and rotations between time-steps, thermal softening, Hugioniot volumetric relationships, strain and strain-rate dependency for elastic-viscoplastic deviatoric behavior, generalized inertial forces, and conductive, convective and radiation heat fluxes. Continuous mapping between fluid and solid states were obtained by selecting velocity and temperature as the primary variables. The resulting set of mass, linear momentum and

DD FORM 1 JAN 73 1473 EDITION OF 1 NOV 65 IS OBSOLETE

Unclassified

SECURITY CLASSIFICATION OF THIS PAGE *(When Data Entered)*

20. Continued

energy equations form a coupled set of differential and integral-differential equations. These equations were approximated by discretizing in both time and space via the method of weighted residuals using piecewise continuous weighting and trial functions. A quadratic time-element was assumed and a wide variety of algebraic recursion relationships were derived for the corresponding implicit solution schemes. In order to "quickly" evaluate any of these solution schemes, a new concept entitled "creation and annihilation" was introduced where geometric sub-regions are added to, and subtracted from, the geometric problem during the penetration process.

A PHYSICAL MODEL AND CONSERVATION EQUATIONS FOR DYNAMIC SOLID-LIQUID BEHAVIOR

John N. Majerus
Mechanical Engineering Department
Villanova University

TABLE OF CONTENTS

For
&I
d
By
Distribution/
Availability Codes
Dist | Avail and/or Special
A-1

TABLE OF CONTENTS (Continued)

LIST OF ILLUSTRATIONS

I. INTRODUCTION

The objective of this research effort is to develop a predictive numerical 2-D model which meets the following twenty-one criteria:

1. Realistically models the geometry and velocity distribution of any stretching rod associated with state-of-the-art self-forging fragments (SSF) and shaped-charge warheads.

2. Geometrically models any zero-obliquity target containing horizontal or vertical layers, multiple materials, free surfaces and possible air spaces.

3. Geometrically formulated so that the stretching rod and target model can be readily extended to oblique impacts.

4. Includes all thermal properties of any rod or non-chemically reactive target-material.

5. Equations-of-state which account for phase changes.

6. Compressible and viscous effects considered for fluids.

7. Elastic-viscoplastic constitutive equation used for solid materials.

8. Strain-displacement relationship includes large rotations and extensions.

9. Primary shocks are included in the model.

10. Time-dependent fracture criteria is used for solid and liquid materials.

11. Temperatures within the solid target and rod can be determined if initial termperatures and convective film coefficients are known.

12. Computation times should be less than 10 minutes for a 2-D penetration process which involves 500 μs of penetration time.

13. Quantitative agreement with existing penetration and penetration vs. time data for shaped-charge jets.

14. Quantitative agreement with data for radial target response for monolithic or layered metallic targets impacted by a stretching rod.

15. Quantitative agreement with experimental phenomenon associated with radial target influence on axial penetration.

16. Qualitatively predicts experimental phenomenon associated with "particle" jets.

17. Qualitatively predicts experimental phenomenon associated with confined columns.

18. Qualitatively predicts experimental phenomenon associated with ejected material.

19. Qualitatively predicts experimental phenomenon associated with heating of target material by a penetrating jet.

20. Qualitatively predicts experimental phenomenon associated with the penetration of brittle hard materials.

21. Qualitatively predicts experimental phenomena associated with the influence of lateral dimensions and confinement upon the behavior of brittle hard materials.

This 2-D model is to be developed over a three-year time-span, and this report presents the results of the effort for the first year.

Obviously, in order to meet the above criteria, one must insure that the pertinent physical parameters are included in the model, and that the laws of physics are included in a consistent manner. Therefore, this work concentrated upon the establishment of a self-consistent set of equations. However, independent and University sponsored research was concerned with the review of state-of-the-art solution techniques used in existing structural and hydrodynamic codes. Since this independent research had a bearing on the development of the equations, the review will be discussed first.

II. OVERALL SOLUTION SCHEME

Recent publications involving non-linear dynamics of solids,[1] the flow of solids during extrusion,[2] numerical heat-transfer,[3] and computational

---

[1] *J. T. Oden and G. F. Carey, FINITE ELEMENTS: SPECIAL PROBLEMS IN SOLID MECHANICS, Volume V of the Texas Finite Element Series, Prentice-Hall Inc., New Jersey, 1984.*

[2] *O. C. Zienkiewicz and P. N. Godbole, "Flow of Plastic and Visco-Plastic Solids with Special Reference to Extrusion and Forming Processes," Int. J. Num. Meth. Engr., 8, 3-16, 1974.*

[3] *O. C. Zienkiewicz and C. J. Parekh, "Transient Field Problems: Two-Dimensional and Three-Dimensional Analysis by Isoparametric Finite Elements," Int. J. Numerical Methods Engr., 2, 61-71, 1970.*

fluid-mechanics,[4] show that the finite-element technique (mathematically known as the Method of Weighted Residuals) can yield good approximations. Most importantly, a "good" approximate solution can be obtained using a relatively small number of judiciously selected "super elements." Also, the problem appears to be well-posed if velocities and/or temperatures are taken as the "essential" boundary conditions, with the stresses, pressure and heat fluxes taken as the "natural" boundary conditions. Hence, these ideas must be kept in mind during the establishment of the self-consistent set of equations.

Figure 1 shows an assumed system associated with one particular region of material. This region of material is similar to a moving control-volume with a time-dependent shape and volume. The volume and shape changes due to both boundary and internal conditions, and possible mass transfer across its boundaries. Note that the applied boundary conditions can involve velocity, and surface pressures (negative tractions) due to detonating explosives. Figure 2 shows a schematic diagram of a region with a sub-region undergoing a phase-transition due to the applied boundary conditions. This phase-transition could be either a thermodynamic transition, e.g., solid to liquid via a melting region,[5] or a polymorphic transition involving the atomic structure of the solid material.[6]

Since the thermal-mechanical-failure properties of the material undergo drastic changes due to either type of phase-transition, the author chose to represent each phase-region of material as a "super-element" of the finite-element approximation. Furthermore, any number of interacting super-elements can be used to represent any particular problem of interest, i.e., a shaped-charge jet impacting a target, or a shaped-charge jet being impacted by another body.

Note that this usage of separate elements for each "phase" region can cause the "creation" and "annihilation" of elements during the penetration process. Mathematically, this is included in all the conservation equations via mass, momentum and energy transfer across the phase-boundary S_{PB} joining two different phase regions. Furthermore, prior to a phase-transition, certain phase regions will belong to a "null-set," i.e., the physical size, mass, momentum and energy are identically zero. Numerically, because of the finite time-steps, the initial zone of a new phase is mapped from the solution at the previous time step, e.g., the geometric locations where $T \geq Tm$. Because of certain discontinuities in volume, and endothermic or exothermic entropy changes, a "refined" phase-zone may be required via an iterative solution at that particular time-step.

---

[4] *A. J. Baker, FINITE ELEMENT COMPUTATIONAL FLUID MECHANICS, Hemisphere Publishing Corp., New York, 1983.*

[5] *L. H. VanVlack, MATERIALS FOR ENGINEERING, Chapters 5 and 6, Addison-Wesley Publishing Co., Reading, Mass., 1982.*

[6] *Ibid, Chapters 2 and 11.*

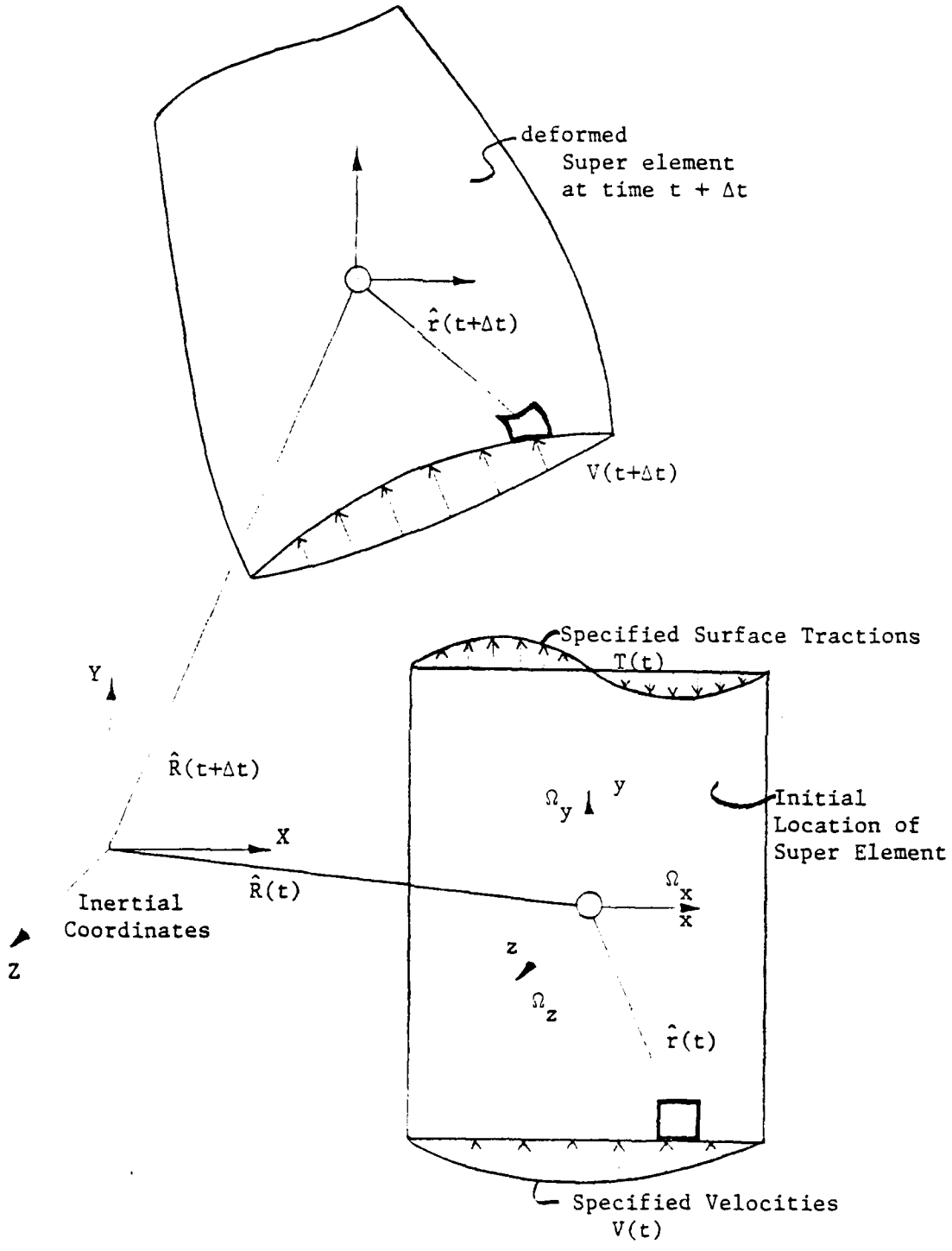

FIGURE 1 Schematic System Associated With One Super Element

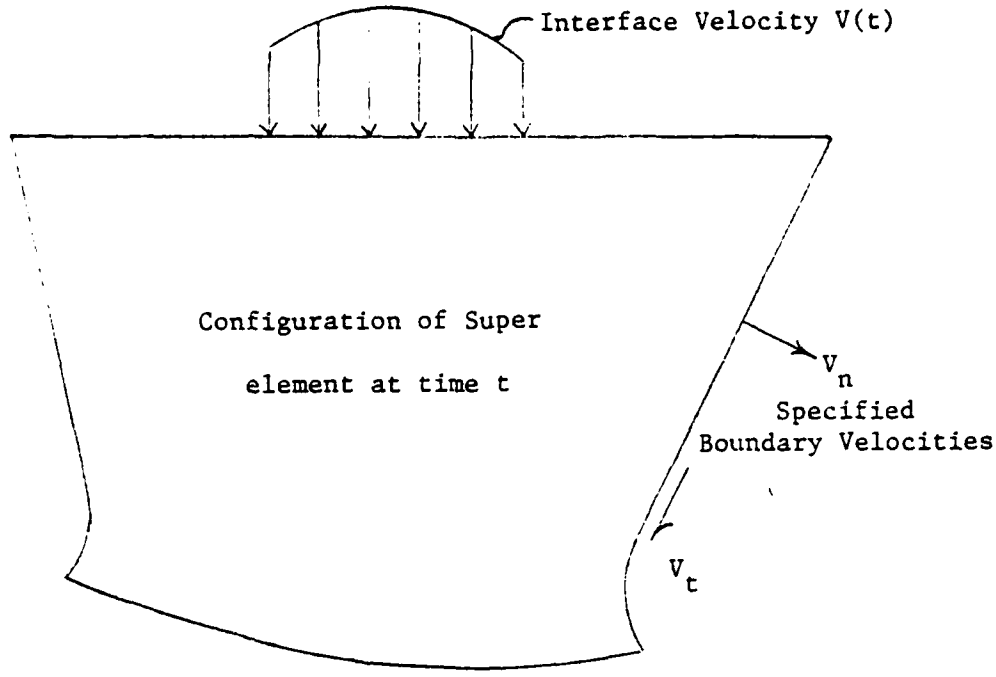

SCHEMATIC OF PHASE CHANGE

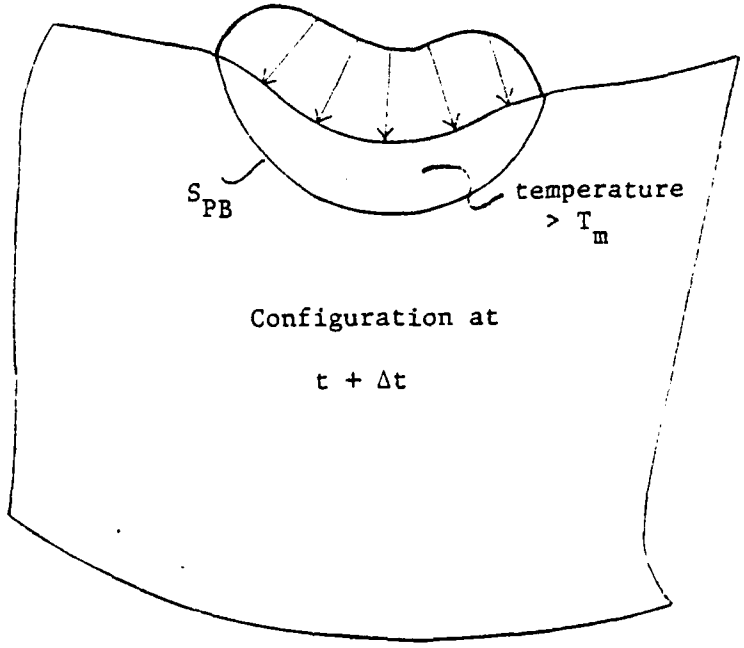

FIGURE 2 Schematic Diagram Showing an Induced Phase Boundary S_{PB} due to Applied Boundary Conditions

The above process of creation and annihilation of elements (hereafter referred to as the "C and A" process) is somewhat similar to the process of "rezoning" used for highly distorted regions in Lagrangian hydrocodes such as HEMP. However, in the C and A process, the mass, momentum and energy of the annihilated material is mapped directly (within the accuracy of the finite-element method) into the created material. Conversely, (to the author's knowledge) the mass, momentum and energy of the highly distorted regions are "lost" during a rezoning process.

It appears that the above C and A process using super-elements differs considerably from current finite-element (hereafter denoted as FE) methods concerned with contact and indentation problems (see review in reference 1). Consequently, a few comments will be made concerning current FE methodology and the proposed extension to the C and A process.

The most commonly used technique for solids involves the displacement formulation which requires a semi-inverse method where the functional form of the displacement solution within the FE region is assumed a priori. However in penetration problems, initial and/or interface velocities are specified, certain velocities are known (usually zero at certain boundaries), fluids can occur within the target and in many problems velocities are the desired quantities. Therefore, the author chose to use a velocity formulation* for the FE model. Because of the large amount of existing radiographic and framing-camera data and various hydrodynamic code calculations, I believe that good initial guesses on velocity distributions can be made. Obviously, if a situation arises where no information exists or the initial guesses prove to be "poor," any material region can be subdivided into numerous interconnected subdomains i.e., more than one super-element. If the solution technique is properly formulated, one should be able to "converge" to a solution of the desired accuracy with respect to a preselected measure of error. Hence the solution technique must contain a consistent "convergence" criteria, and this is currently being studied via independent and University-funded research.

As will be pointed out later, the Method of Weighted Residuals, as implemented by the FE Method, involves the solution of a simultaneous set of non-linear algebraic equations, whose degree of non-linearity depends upon the magnitude of the deformations and the constitutive equation for the material. The review indicated that the most popular method of solving this set of equations is the following approach:

a. drop all non-linear terms and solve the simultaneous linear set
b. add the first non-linear term to the set of equations, in the previous linear solution and then iterate until a certain criteria of convergence is achieved

---

*Displacements are kinematically related to the velocities via a simple time-integration over the velocity history.

c. add the next non-linear term to the set of equations and repeat step b
d. continue the above approach until all non-linear terms have been accounted for.

The advantage of the above approach is that the addition of the non-linear terms can be controlled by the user. Hence, numerical experiments can be conducted to ascertain the importance of the various non-linear contributions and those deemed of lower-order contributions can be "turned-off" by the user. Therefore, the user can do a trade-off between accuracy of solution and the amount of computer time it takes to achieve an approximate solution. It appears that nodal velocities are an appropriate measure of error for usage in the above iteration-scheme, and this will be investigated during the second year of research.

A disadvantage of the above FE method is that the iterative solution of simultaneous equations is a slow process when there is a large number of unknowns in the so-called bandwidth or wavefront. Furthermore, numerical fluid-mechanics studies (see review in reference 4) have shown that, for the same number of unknowns, it takes longer to solve a system of super-elements (so-called quadratic or cubic elements) than a larger system of linear elements (such as used in the EPIC and DYNA3D programs). Conversely, application of a few super-elements to solid mechanics problems[7,8] have produced "quicker" solutions when the problem is properly formulated.[4,9] Therefore, a system consisting of a few judiciously selected super-elements should provide "quick" approximate solutions.

Historically, numerical solutions involving shaped-charge jet penetration necessitate a large number of zones or elements because of the smallness of the jet (order of mm) compared with the target thickness (hundreds of mm). Furthermore, very large velocity-gradients occur in a small region (order of the penetrator-diameter) around the moving penetrator/target interface. This poses a dilemma in that our "few judiciously selected super-elements" cannot *a priori* model this condition.

It appears to the author that the following approach depicted in Figures 3 through 7 offers a way around both the above dilemma, and for implementing the C and A process. First, we recognize that the vast majority of most targets undergo linear behavior in lateral regions which are on the order of several hole diameters away from the path of the penetrator. Hence, these outer regions could be modeled using a few super-

---

[7] *O. C. Zienkiewicz, THE FINITE ELEMENT METHOD IN ENGINEERING SCIENCE, Chapter 9, McGraw-Hill, London, 1971.*

[8] *L. J. Segerlind, APPLIED FINITE ELEMENT ANALYSIS, Chapters 14-16, John Wiley & Sons, Inc., New York, 1976.*

[9] *G. F. Carey and J. T. Oden, FINITE ELEMENTS: A SECOND COURSE, Volume II in the Texas Finite Element Series, Chapters 1 and 2, Prentice-Hall, Inc., New Jersey, 1983.*

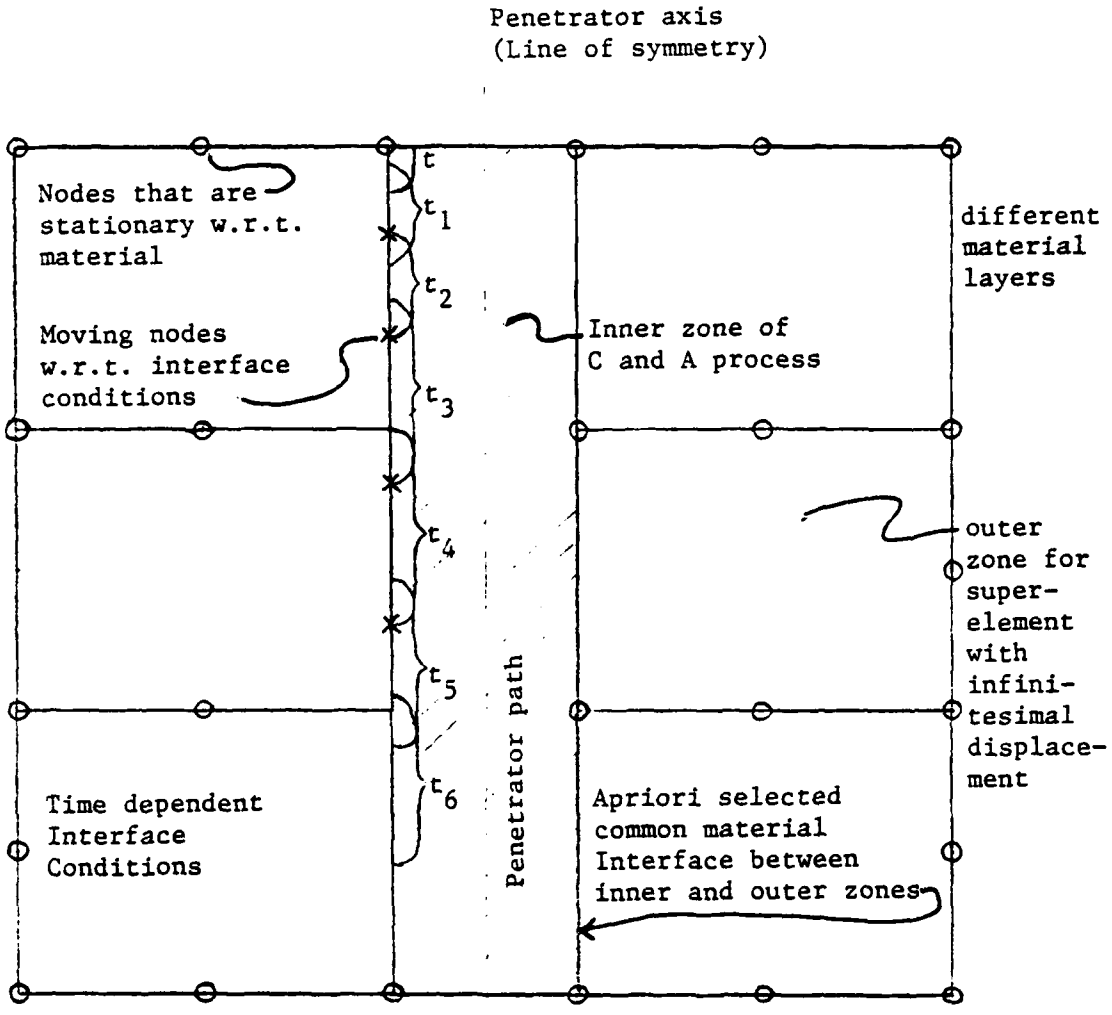

FIGURE 3 Overview of Target Definition Using Super-Elements and the C and A Process

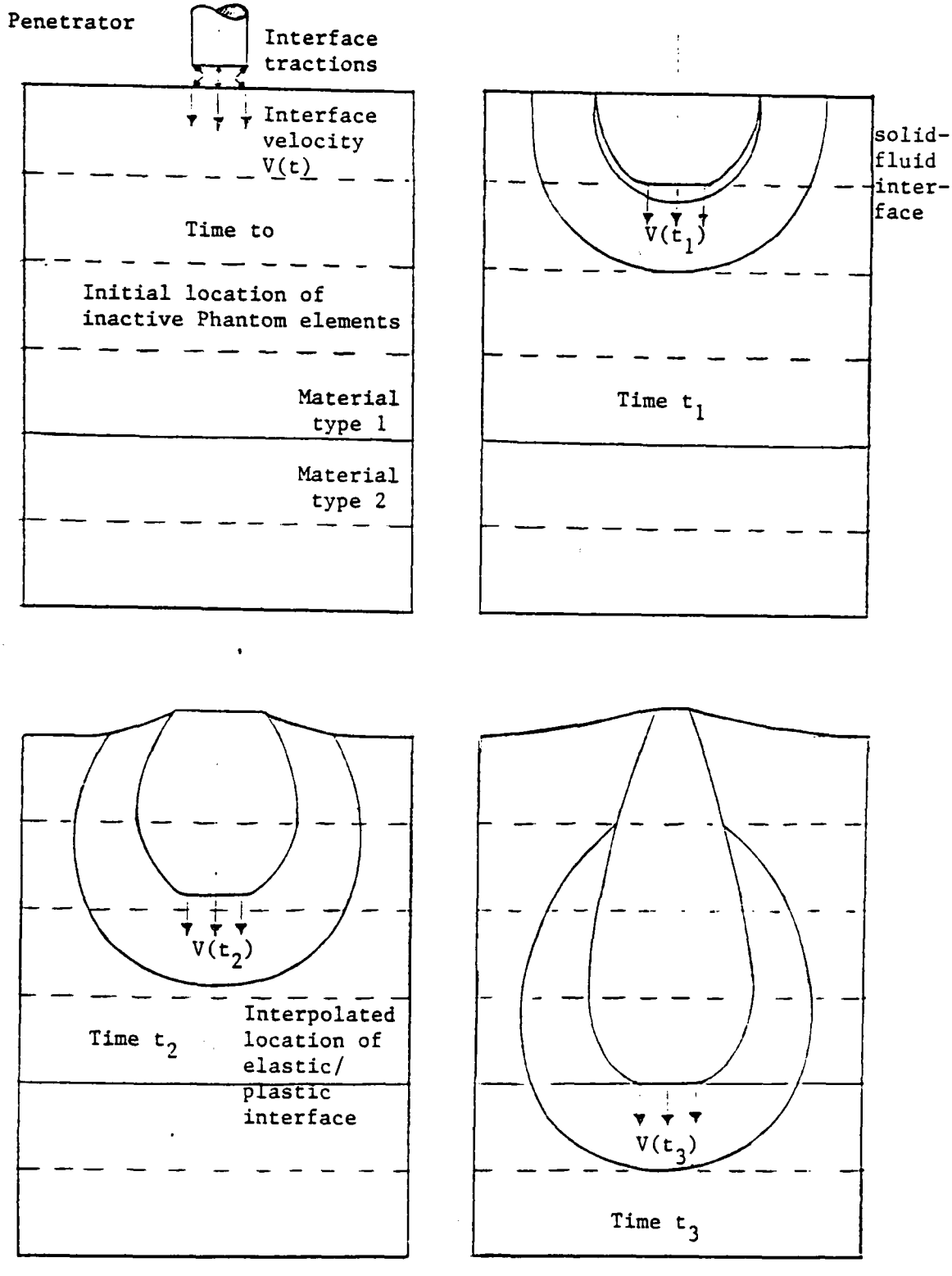

FIGURE 4 Schematic Overview of Deformations at Three Different Times

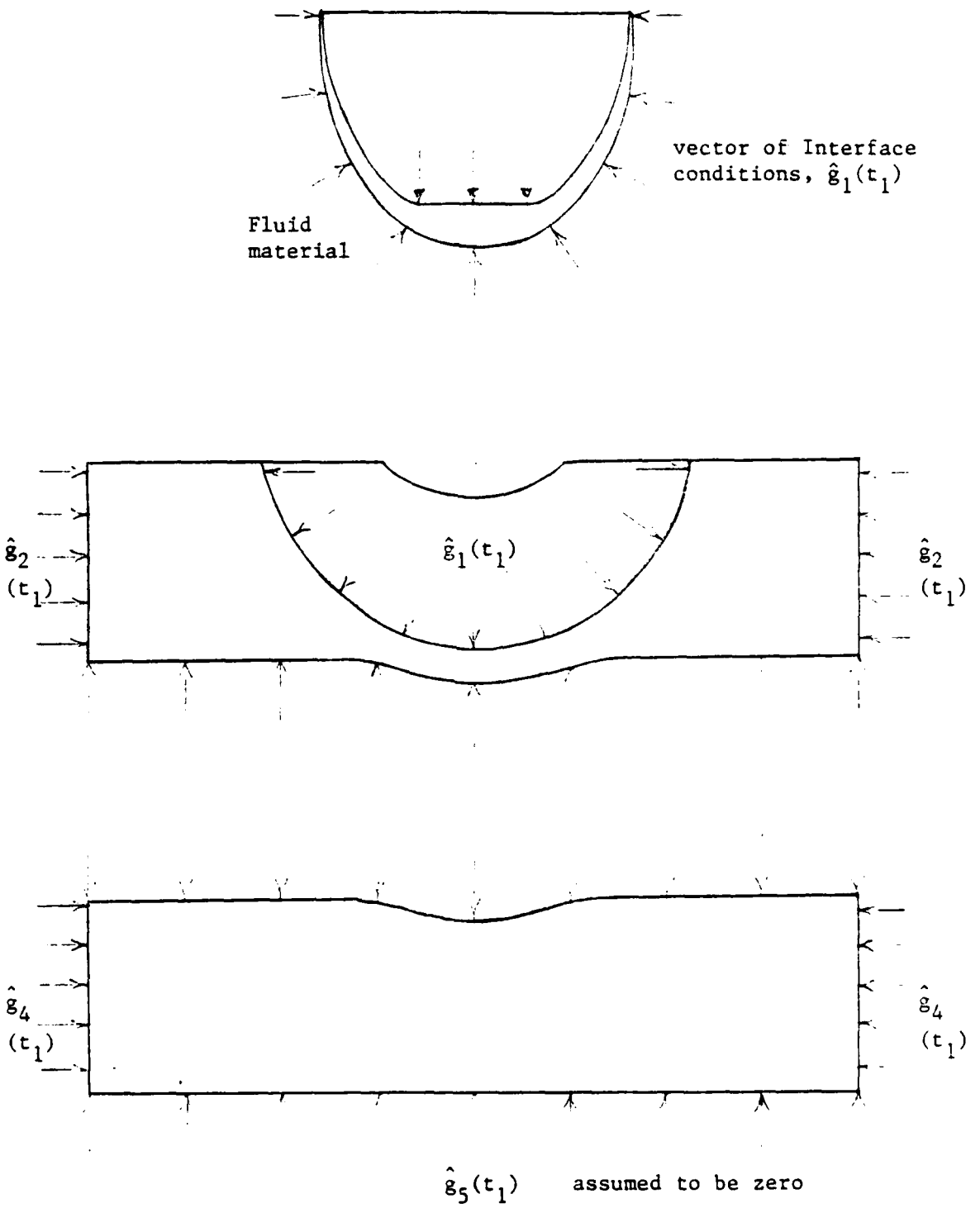

FIGURE 5 Active Elements at Time t_1
Showing the Interface Vector-Functions $\hat{g}(t)$

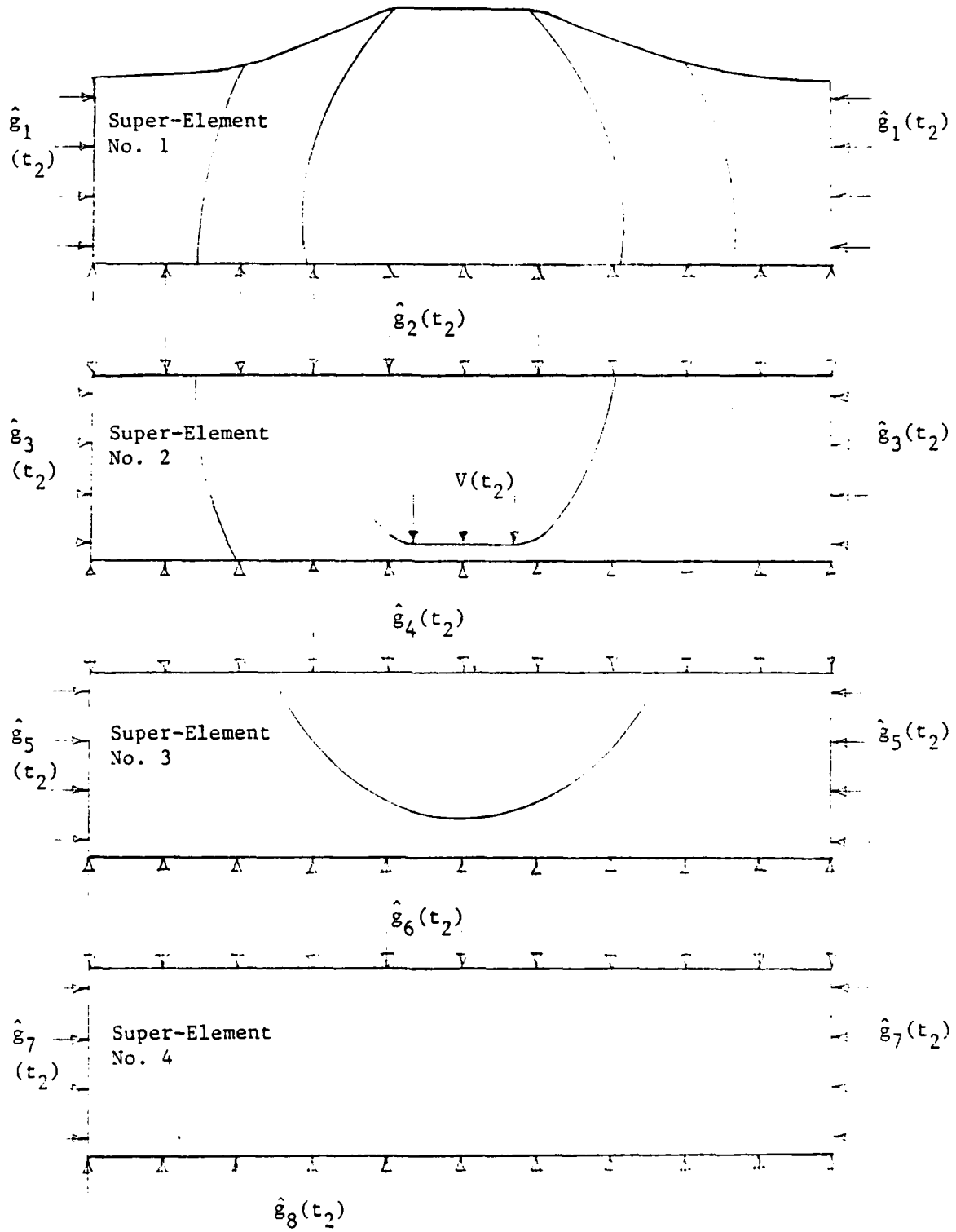

FIGURE 6 Active Elements at Time t_2
Showing the Interface Vector-Functions $\hat{g}(t)$

Super-Element no. 1 is removed from inner region iteration process when $\hat{g}_2(t_2) \cong 0$

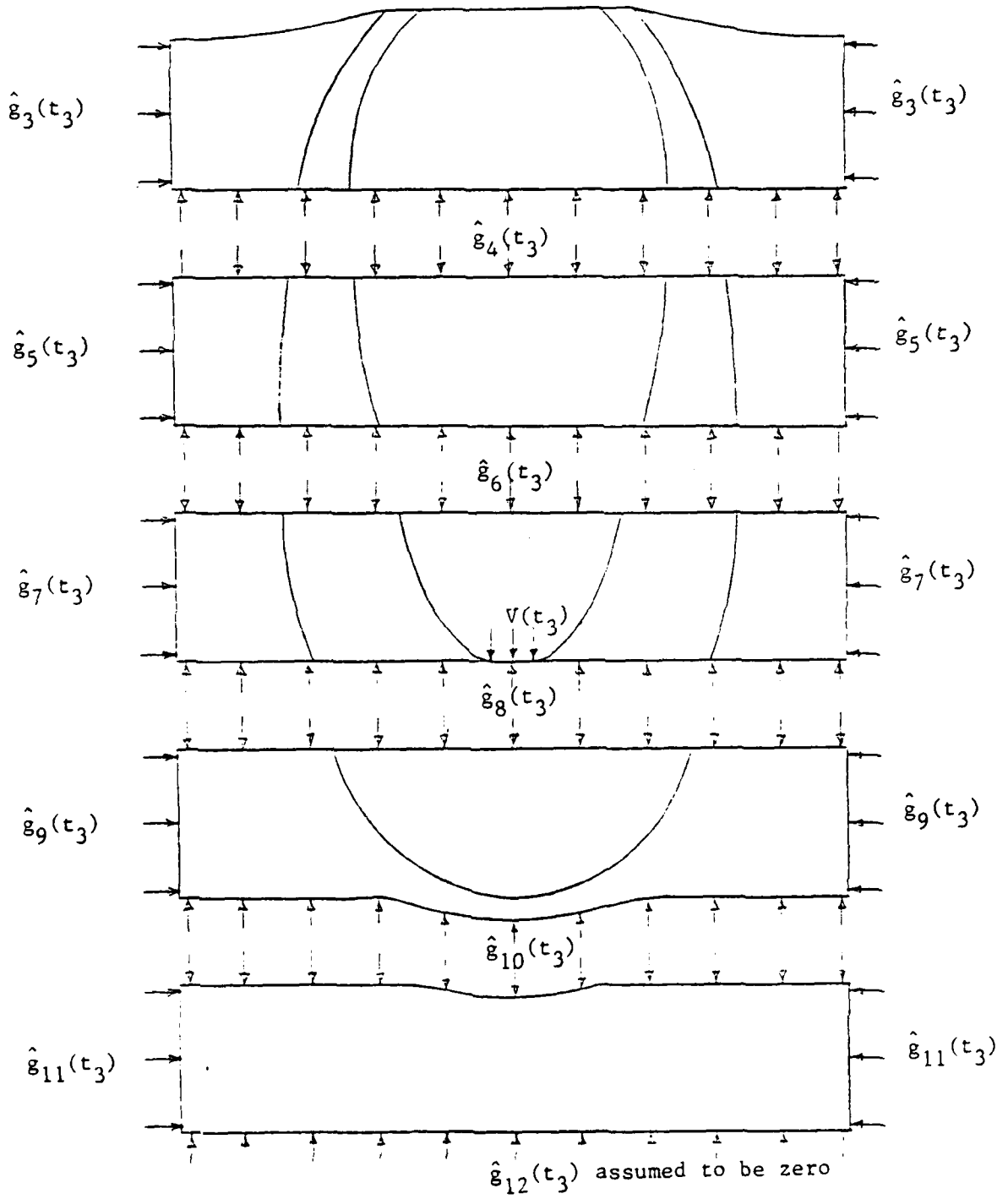

FIGURE 7 Active Elements at Time t_3
Showing the Interface Vector-Functions $\hat{g}(t)$

elements on either side of the penetrator-path. Furthermore, the algebraic equations are essentially linear for the FE unknowns within these regions. Secondly, the "inner" region along the path of the penetrator is the only region for the highly non-linear C and A process. Hence, the non-linear formulation is applied only to this "inner" region. Thirdly, the inner and outer regions communicate only via the matching of velocities, tractions, temperature and heat-fluxes along the common interface (see Figure 3). This matching must be done in an iterative fashion, but does not have to be done at each time-step. Fourthly, the C and A process progresses along the penetrator-path in some fashion with the penetrator/target interface, and downstream material does not sense the penetration process until an elastic or plastic stress-wave arrives (see Figure 4). Figures 5 through 7 illustrate how inner super-elements become active, i.e., must be included in the simultaneous iterative solution, whereas other inner super-elements become inactive, with the motion of the penetrator/target interface. Note that this active/inactive process is exactly analogous to the C and A process, and all iterative interfaces can be analyzed by the same method.

Numerically, the above C and A process appears to offer several advantages over current FE methodologies. First, a priori knowledge of the initial location and material associated with each phantom super-element allows the user to "turn-on" the appropriate non-linearities within each element, which in general can differ from element to element. This could permit a substantial savings in computational time.

Secondly, it is numerically faster to solve N sets of M number of simultaneous equations associated with each super-element, than the N*M simultaneous equations associated with all N super-elements. Since an iterative solution must be obtained regardless of the number of simultaneous equations, minimal solution times should exist for certain choices of N and M. Therefore, a trade-off should exist between the number of preselected phantom super-elements and the number of nodes associated with each super-element.

Thirdly, since the outer super-elements and each inner super-element is analyzed or "processed" separately, considerably "faster" solutions are possible by using computers with multiprocessors. For example, a co-processor or a parallel processor could be used to run the inner and outer regions, which "talk to each other" after a preselected number of iterations or time-steps. This may be extremely important in the near future since the next generation of "super computers" are purported to be based upon a large number of interconnected processors.

III. DEVELOPMENT OF THE PHYSICAL MODEL

Now that the flavor of the solution scheme has been presented, we can progress to the assumptions associated with the selected physical model. The corresponding self-consistent set of equations must include the conservation laws of physics and chemistry, the basic principals of thermodynamics and materials science, and the basic postulates of continuum mechanics. Presently, the model will assume no chemical reactions and hence chemical considerations will be neglected. Also, the model neglects all electromagnetic forces and energy, contains no failure or fracture criteria, nor any consideration of solution bifurcations, i.e., buckling phenomena is not considered explicitly.

As indicated in Figure 1, both the global inertial coordinate and the attached local, fixed, coordinate systems are chosen to be rectangular Cartesian coordinates. Hence, all the equations will be written and derived with respect to these coordinates. Application to other types of coordinate systems can be done using the rules of calculus transformations. Note that, while the local coordinate system is attached to some material point in the system which moves globally according to the position vector R(t), the direction of the axes always corresponds to the direction of the global axes.

Also attached to the material system is a curvilinear material (so-called Lagrangian) coordinate system initially parallel to the rectangular Cartesian system, but which deforms with the material. Furthermore, each super-element has its own local coordinate system used for calculations. After each calculation, the actual location of the total material system can be obtained by mapping back to the inertial coordinate system, and this yields the updated nodal locations. It is this mapping to the actual location that permits one to observe any possible penetrator/target interactions away from the frontal interface.

Using these coordinates and including the possibility of phase transitions, conservation of mass yields the equation presented in Appendix A. This equation is satisfied (within the accuracy of the mesh or grid) by using the updated Lagrangian coordinates and the previously discussed C and A approach.

In order to derive the remaining equations, we must decide on the magnitude of the deformations that occur between time-steps. The usual infinitesimal form of the conservation equations requires extremely small time-steps for a penetration problem, i.e., on the order of 10^{-1} to 10^{-2} μs. This would require a large amount of CPU time for a FE solution to a realistic problem. Therefore, since relatively large time-steps (order of μsec) are desirable, finite deformations are quite possible between time-steps. Hence, large deformation theory[19] will be

[19] *V.V. Novozhilov, THEORY OF ELASTICITY, pp 18-88, translation of Russian book TEORIYA UPRUGOSTI (1958), Israel Program for Scientific Translation, OTS61-11401, Jerusalem, 1961.*

utilized in the current model and introduces geometric sources of non-linearity. However, the advantage of large deformation theory is that the geometric deformations do not force one to use small time-steps in the solution. Rather, the size of the time steps is dictated by either: a. the time variation of the boundary conditions, or b. the user's interest in short time behavior, i.e., "shock propagation."

Several assumptions must be introduced into the large deformation theory in order to simplify the elemental form of the conservation equations. These assumptions involve the size of the extensions and shears that occur between the time steps. This size is assumed to be finite but small compared to unity and one radian respectively. Note that the theory considers material rotations which could be larger than either the extensions or the shears. Previous hydrocode and experimental observations indicate that a material "particle" can undergo considerably large rotations at the target/penetrator interface region, and hence no limitations* were applied to the material rotations. The author believes that the extension and shear assumptions are not severely limiting because, for a stretching rod, these assumptions apply as long as the following two conditions** are satisfied:

$$\text{Small extensions} \rightarrow \frac{\Delta t}{t_{OB}} << 1$$

$$\text{Small shears} \rightarrow \left[1 + \frac{\Delta t}{t_{OB}}\right]^{3/2} \cong 1 \rightarrow \frac{\Delta t}{t_{OB}} << \frac{2}{3}$$

where Δt = time-step size,

t_{OB} = time of the calculation as measured from the jet-formation time.

Using the above assumptions, the linear momentum equation takes the form given in Appendix B. The body force terms are written in the expanded form since this permits a visual interpretation of the various contributions, and is easier to write in FORTRAN. Also, the inertial (body) forces includes all forms associated with rotational and translational motion of the local coordinate system.

Note that, if the body forces or surface tractions are either uniform or symmetrical with respect to the local coordinate system, a geometric symmetry with respect to the same axis will yield a zero contribution for

*Rotations ω of the vectors are considered during time-steps, but their magnitudes must be such that $\tan[\omega(t + \Delta t) - \omega(t)] \cong [\omega(t + \Delta t) - \omega(t)]$.

** These conditions stem from the assumption that the radial displacement rate at the interface is of the same order as the rate of penetration. Also it is assumed that the Cauchy stress is approximately equal to the first Piola-Kirchhoff stress.

the corresponding volume or surface integral. Also, many of the volumetric integrals will yield geometric terms, such as the polar moments of inertia, when the other integrands are constant over the volume.

Appendix C gives the development of the three equations associated with the conservation of angular momentum. Note that, whereas the pointwise form of the angular momentum equations are identically satisfied whenever the linear momentum equations are satisfied, the weighted integral form requires additional symmetry conditions. Therefore, these angular momentum equations could be satisfied by either assuming that these symmetry conditions are fulfilled by the deformation conditions, or, by solving for the additional unknowns.

The last conservation equation involves energy and is developed in Appendix D. Because of the assumed general behavior, this equation is quite complex even though only one new variable (temperature) is introduced. Furthermore, since stored thermal energy is required, some form of thermodynamic equation-of-state (hereafter denoted as EOS) must be selected. Since temperature is the critical variable in the C and A process, all thermal-mechanical properties will be assumed to be known functions of temperature T. References 11-13 give some typical types of analytical functions used for these properties.

Several new terms which appear in the energy equation are the strains ε_{ij}, the heat sources Q per unit mass, and the volume fractions f_p and f_e. Because of the possibility of large deformations, the strain-displacement (U_i, U_j, U_k) relationship is

$$\varepsilon_{ij} = \frac{1}{2}\left(\frac{\partial U_i}{\partial x_j} + \frac{\partial U_j}{\partial x_i} + \frac{\partial U_k}{x_i}\ \frac{\partial U_k}{\partial x_j}\right) \qquad (1)$$

where i, j, k = 1, 2, 3 and repeated indices indicates summation. The heat source term is associated with the latent heats corresponding to thermodynamic and polymorphic phase-changes within the material. Most of these latent heats can be obtained from solid-state reference books. The volume

---

[11] *S. K. Godunov, A. F. Demchuk, N. S. Kozin and V. I. Mali, "Interpolation Formulas for Maxwell Viscosity of Certain Metals as a Function of Shear-Strain Intensity and Temperature," translated from Zhurnal Prikladnoi Prikladnoi Mekhaniki i Tekhnicheskoi Fiziki (1974), Plenum Publishing Corp., 1976.*

[12] *G. E. Duvall and D. P. Dandekar, "Theory of Equations of State: Elastic-Plastic Effects II," USA Ballistic Research Laboratories Contract Report No. 106, May 1973.*

[13] *H. B. Callen, THERMODYNAMICS, Appendices D and E, John Wiley and Sons, Inc., New York, 4th Printing, 1963.*

fractions f_p and f_e refer to the percentage of "plastic" work that is irreversible and reversible, with many processes yielding f_e of only a few percent.[5] However, this small percentage may be important in some problems.

The two remaining items that must be selected are the specific forms of the EOS, and the constitutive equation that relates stress σ_{ij} to the other variables.

A. Thermodynamic Equations of State

It appears that most hydrocodes use an explicit volume-dependent form of the solid EOS, such as LASL's equation[14]

$$P(\rho) = P_H(\rho) + \gamma_S \rho \text{ (Internal Energy} - I_H) \tag{2}$$

where

$P_H(\rho) = \rho C^2 X/\{1 - X(S-1)\}^2$,

U_S = Shock Velocity = $C + SU_p$,

U_p = particle velocity = $\bar{v}$,

$X = (\rho/\rho_o) - 1$,

γ_S = Grüneisen coefficient,

$I_H = \frac{1}{2}\left\{\frac{CX}{(\rho/\rho o)-SX}\right\}^2$, C = Intercept of the U_s versus U_p data-line,

ρ = density in the deformed state, $P(\rho)$ = pressure,

ρ_o = reference density, S = slope of the U_s versus U_p data-line.

Conversely, many of the elastic-plastic codes use a Mie-Gruneisen or Cristescu form[15] which explicitly includes the influence of temperature, i.e.,

$$P(\rho,T) = P_H(\rho) + H_0(\rho,T) + H_1(\rho)T^2 \tag{3}$$

---

[14] F. H. Harlow and A. A. Amsden, FLUID MECHANICS, A LASL MONOGRAPH, Los Alamos Scientific Laboratory, Report No. LA-4700, June 1971.

[15] N. Cristescu, DYNAMIC PLASTICITY, Chaps 8, 10, North-Holland Publishing Co., John Wiley and Sons distributors, 1967.

where $H_0(\rho,T)$ and $H_1(\rho)$ depend upon the atomic model[16-19] used to represent the solid state.

Our EOS must include other phases, and presently there appears to be two choices for multi-thermodynamic phase EOS: the Tillotson[17] interpolation equation, or one of the various forms of the GRAY[18] equation. Tillotson's equation is a two-phase equation based upon a Thomas-Fermi-Dirac atomic model (five parameters) for a solid (condensed) state, and the vaporized (isentropically expanded) material is represented by a two-parameter equation which interpolates between the solid state and an ideal gas. GRAY is a three-phase equation for metals based upon a variety of physical models and interpolation equations (see review in reference 19).

Neither the GRAY nor the Tillotson equations contain polymorphic phase-changes.* (But the author believes that these changes can be included by using a dual Hugoniot for $P_H(\rho)$, with a possible volume discontinuity between the dual Hugoniot relations.) Cristescu discusses this behavior in reference 15, and some specific examples will be considered during the research effort of the second year.

Since BRL personnel have used the GRAY equation, and have already generated the critical thermodynamic constants associated with the liquid-vapor, mixed-phase region for seventeen materials,[19] the author selected the GRAY form of the EOS. After reviewing the derivations contained in reference 19, it appears that there are two "implicit" assumptions contained within the equations for the solid region. These assumptions are: a. the initial temperature of the solid is considerably above the Debye temperature T_D, and b. the energy depends only on the thermal and volumetric stored energies. Since T_D could be well above room temperature (see discussion in reference 11) the first assumption is removed from the solid EOS by replacing the "3R' "

---

[16] *J. de Beaumont and J. Leygonie, "Vaporization of Uranium after Shock Loading," Proceedings of the Fifth Symposium (International) on Detonation, Pasadena, California, ACR-184-, pp 547-553, August 18-21, 1970.*

[17] *J. H. Tillotson, "Metal Equations of State for Hypervelocity Impact," General Atomic Report GA-3216, July 1962.*

[18] *E. B. Royce, "GRAY, A Three-Phase Equation of State for Metals," Lawrence Livermore Laboratory, UCRL-51121, September 1971.*

[19] *J. F. Lacetera, "BRLGRAY: The Ballistic Research Laboratory Version of the GRAY Equation of State," U.S. ARRADCOM Ballistic Research Laboratory Technical Report ARBRL-TR-02268, August 1980.*

*The HEMP USER's MANUAL, Lawrence Livermore Laboratory report UCRL-51079 Rev. 1, Dec 1973, indicates a "five-part multiphase equation of state," which appears to be for possible polymorphic phase-changes since the "phases" are determined only by the range of the density change X.

terms by the more general expression $\int_o^T c_v(T)dT/W_A$

where,

$c_v(T)$ = Temperature-dependent coefficient of specific heat for $T \leq T_D$

R' = Universal Gas Constant R/Molecular weight W_A

Limit $c_v(T) \cong 3R$.
$T \to T_D$

The second assumption can be avoided by not using the Grüneisen-like equation with parameter $\Gamma(T,V)$,* but rather by using the Hugoniot definitions (Equations 5, 6, 7 and 9 in reference 19) with the above modified solid EOS. Therefore, the solid EOS takes the following form,

$$E_s(T,\rho) = E_{01}(\rho) + E_{0H} + \int_o^T \frac{c_v(T)}{W_A}\, dT + \frac{G'T^2}{2}$$

$$P_s(T,\rho) = P_H(\rho)\,[1-\gamma_s(V)X/2] + \gamma_s(V)\rho\, E_{01}(\rho)$$

$$+ \gamma_s(V)\rho \int_o^T \frac{c_v(T)dT}{W_A} + \frac{1}{2}\,\gamma_e\,\rho G'T^2$$

where

E_{0H} = assumed by the present author to be the linear elastic bulk-behavior at T_D, i.e., $3\kappa(T_D)\int_o^T \alpha(T)dT/\rho(T_D)$,

$\kappa(T_D)$ = elastic bulk-modulus coefficient,

$\alpha(T)$ = unidirectional coefficient of thermal expansion,

$E_{01}(\rho)$ = Royce's approximation-function

$$\frac{C^2X^2}{2(1-SX)}\left\{1 + \frac{S}{3}X + \frac{S^2}{6}\left(1-\frac{\lambda_o}{S}\right)X^2\right\} + E_\infty\,(1+\lambda_o X),$$

λ_o = Lattice constant,

$E_\infty = E_{0H} - E_S\,(T=0^oK,\ \rho_o)$,
(reference 19 uses $-T_D\ \{3*8.134*10^{-5}+150G'/W_A\}$),

---

* It appears that this term is never used in reference 19, but merely represents a formal correction term to a Grüneisen-like EOS for a solid.

G' = atomic-weight scaled electronic energy coefficient,

$= \pi^2 N_e K R'/2E_f$,

$g_e = W_A G'$,

K = Boltzmann's constant,

N_e = number of free electrons,

E_f = Fermi Energy,

$= 26 (N_e \rho_o/W_A)^{2/3}$,

$\gamma_s(V)$ = linear volume-dependent Grüneisen coefficient,

γ_e = electronic gamma (reference 19 assumes $\gamma_e = 2/3$ whereas references 15 and 16 assume $\gamma_e = ½$).

With the above modified form of the solid EOS, we can use the remaining GRAY phase-equations,

a. Two-Phase Melt Region

$$E_m(T,\rho) = E_s(T,\rho) + \nu\{T - \nu(\Delta T/2)\}(\Delta S' - 0.143R')^*$$

$$P_m(T,\rho) = P_s(T,\rho) + \nu\lambda T_m \rho(\Delta S' - 0.143R')^*$$

where,

$\Delta S'$ = entropy of melting/W_A,

$\nu = \{T - T(\rho)\}/\{T_\ell(\rho) - T_s(\rho)\}$,

$\Delta T = T_\ell(\rho) - T_s(\rho)$,

$T_m = \{T_s(\rho) + T(\rho)\}/2$,

$T_s(\rho)$ = solidus temperature,

$T_\ell(\rho)$ = liquidus temperature,

λ = coefficient of the Lindemann Law,

$= d(\ln T_m)/d(\ln \rho)$

---

*In reference 19, the ΔS and R terms appear without the "primes," but the primed quantities are necessary for extrapolation to the solid state, and because of the stated "scaled entropy of melting."

b. Liquid-Phase Region

$$E_\ell(T,\rho) = E_s(T,\rho) + T_s \ \Delta S' + 0.143R' \ \Delta T/2 + \frac{3R'}{2\bar{\alpha}} T_m \ A(T),$$

$$P_\ell(T,\rho) = P_s(T,\rho) + \lambda T_m \ \rho\Delta S' + \frac{3R'\lambda}{2\bar{\alpha}} \rho T_m \ A(T),$$

where,

$$A(T) = \ln\{(\bar{\alpha}T/T_m) + 1\} - (1+\bar{\alpha})\ln(1+\bar{\alpha}) - \bar{\alpha}\{(T/T_m) - 1\}$$

$\bar{\alpha}$ = fitting parameter for liquid specific heat; reference 19 uses $\bar{\alpha} = 0.1$.

c. Vapor-Phase Region

$$E_v(T,\rho) = E_s(T,\rho) + 3R'T/2 - 2R'T^2\rho\{(2-\eta)/(1-\eta)^3\}\frac{dV_b}{dT} - a_y\rho,$$

$$P_v(T,\rho) = R'T\rho\{(1+\eta+\eta^2-\eta^3)/(1-\eta)^3\} - a_y\rho^2,$$

where,

$\eta = \rho V_b(T)$,

V_b = vapor-exclusion volume,

a_y = coefficient of the attractive potential,

$dV_b/dT = -V_b/(4T)$.

Obviously, the above equations of state cannot be used until a large amount of information is known about a material. Also reference 19 presents a program for estimating the critical constants associated with the liquid-vapor mixed-phase regions, and these constants are required in order to use the previous equations for a general mixed-phase condition.

We now need to develop a constitutive equation which is applicable to both solid and fluid behavior.

B. Constitutive Equation for "Hygrosteric" Materials

An excellent review of constitutive equations for "plastic" solid-behavior is given in reference 15. However, irrespective[20] of the temperature dependency of the material parameters, these equations do not take the classical Newton-Cauchy-Poisson fluid-equation form

$$\hat{\sigma} = -p\hat{I} + \lambda(\text{tr } \hat{A})\hat{I} + 2\mu_f \hat{A} \qquad (4)$$

where,

$\hat{\sigma}$ = stress tensor,

$\hat{I}$ = identity matrix,

p = hydrostatic pressure,

$\hat{A}$ = matrix with components $A_{ij} = \frac{1}{2}(\partial V_i/\partial X_j + \partial V_j/\partial X_i)$,

λ, μ_f = material parameters.

This poses a problem since we would like a constitutive equation which continuously maps the material behavior between the solid and liquid states. Noll[21] discusses the concept of a "hygrosteric" material which can take either solid or fluid-like behaviors. Depending upon the functional assumptions, the hygrosteric constitutive equation for an isotropic material can be written as a general function[21] of the strain invariants (I_1, I_2 and I_3), and various powers of (tr $\hat{A}$). Any general function of this form satisfies all the restrictive conditions[20-22] associated with the mathematical consistency of continuum mechanics. Also, an acceptable form of the constitutive equation involves the decomposition of stress $\hat{\sigma}$ into a volumetric component $p\hat{I}$, and the so-called "extra" stresses $\hat{S}$.

Of all the equations[23] that satisfy the above general forms, the author selected the simplest, i.e.,

$$\sigma_{ij} = \{-P(T,\rho) + \kappa(T)(\sqrt{I_3}-1)^* - 3\kappa(T)\alpha(T)(T-T_D)\}\,\delta_{ij} + s_{ij} \qquad (5)$$

---

*For small strains, $(\sqrt{I_3}-1) \rightarrow \varepsilon_{11}+\varepsilon_{22}+\varepsilon_{33} \equiv \varepsilon_{kk}$

[20] C. Truesdell, "Elasticity and Fluid Dynamics," J. Rational Mechanics and Analysis, 1, 126-262, 1952, and Vol 2, 593-611, 1953.

[21] Walter Noll, "On the Continuity of the Solid and Fluid States," J. Rational Mechanics and Analysis, 4, 3-81, 1955.

[22] Walter Noll, "A Mathematical Theory of the Mechanical Behavior of Continuous Media," Archives Rational Mech. Analysis, 2, 198-226, 1958.

[23] Proceedings of the International Conference on Constitutive Laws for Engineering Materials: Theory and Application, Tucson, Arizona, Jan, 1983.

where the {...} terms refer to the total volumetric component, and $P(T,\rho)$ represents the EOS pressure component. Equation (5) passes in the limit $(T \to T_\ell(\rho))$ to Equation (4) if the extra, or deviatoric, stresses s_{ij} depend upon the velocity gradient A_{ij} when $T \to T_\ell(\rho)$. This can be accomplished by using a modification of Perzyna's constitutive equations[24] for rate-sensitive materials and Zienkiewicz and co-workers used this approach in references 3 and 25.

Perzyna introduced a plasticity function $\Phi(F)$ which satisfies the conditions

$$\begin{aligned} \phi(F) &= 0 \text{ when } F < 0 \\ \phi(F) &\neq 0 \text{ when } F > 0 \end{aligned} \tag{6}$$

where F = Prager's dynamic overstress-function

$$= \left(\sqrt{I_s^{(2)}}\right)/K(T) - 1$$

$I_s^{(2)}$ = second invariant of the extra stress-tensor

$$= \tfrac{1}{2}\, s_{ij}\, s_{ij},$$

K(T) = "yield stress" in simple shear.

Note that K(T) can also be a function of hydrostatic pressure, effective deviatoric strain $I_e^{(2)} \equiv \tfrac{1}{2}\, e_{ij}\, e_{ij}$,* and/or effective deviatoric strain-rate $I_{\dot{e}}^{(2)} \equiv \tfrac{1}{2}\, \dot{e}_{ij}\, \dot{e}_{ij}$.

Cristescu and Predeleanu[15] manipulated Perzyna's equations into the following form for loading conditions ($\{\sigma_{ij}\, \dot{\epsilon}_{ij} + \dot{T}\, \partial\Phi/\partial T\} > 0$) and an "elastic viscoplastic" body,

---

*By definition, $e_{ij} = \epsilon_{ij} - \delta_{ij}\, (\sqrt{I_3} - 1)/3$.

[24] P. Perzyna, "The Constitutive Equation for Rate Sensitive Plastic Materials," Quarterly Appl. Math., XX, No. 4, 321-322, 1963.

[25] O. C. Zienkiewicz, P. C. Jain and E. Onate, "Flow of Solids During Forming and Extrusion: Some Aspects of Numerical Solutions," Int. J. Solids Structures, 14, 15-38, 1978.

$$s_{ij} = (1 + \delta_{ij})^{*} G\, e_{ij} \quad \text{if } J \le K(T)^2,$$

$$= (1 + \delta_{ij})^{*} \{G_T(e_{ij} - e_{ij}^{E}) + \eta_{eff}(\dot{e}_{ij} - \dot{e}_{ij}^{E})\} \quad \text{if } J > K(T)^2, \tag{7}$$

where G = shear modulus,

$$J = \tfrac{1}{2}\{(1 + G_T/G)s_{ij} - (1 + \delta_{ij})^{*} G_T e_{ij}\}^2,$$

$\dot{e}_{ij}^{E} = \dot{s}_{ij}/(1 + \delta_{ij})^{*} G$,

e_{ij}^{E} = values of e_{ij} satisfying $J = K(T)^2$,

G_T = strain-hardening shear modulus

and viscosity η_{eff} is a non-linear function of stress, strain, strain-rate and material properties. For unloading, the stresses must satisfy the inequality $(\sigma_{ij}\dot{\varepsilon}_{ij} + \dot{T}\partial\Phi/\partial T < 0)$, whereas relaxation implies that $(\sigma_{ij}\dot{\varepsilon}_{ij} + \dot{T}\partial\Phi/\partial T = 0)$.

Equation (7) satisfies both the solid and fluid equations if the effective viscosity is written (assuming a rule-of-mixtures) as,

$$\eta_{eff} = f_f\eta_f + f_s\eta_s \frac{\sqrt{J}}{K(T)\Phi(\bar{F})}, \tag{8}$$

where f_f = volume fraction of fluid,

f_s = volume fraction of solid,

$\bar{F} = (\sqrt{J}/K) - 1$,

η_f = fluid-viscosity,[26] which can be a function of temperature, effective deviation strain $I_e^{(2)}$ and effective deviatoric strain-rate $I_{\dot{e}}^{(2)}$,

η_s = solid-viscosity,[11] which can be a function of temperature and the strain-hardening function J,

---

*Because of the strain ε_{ij} definition, $(1 + \delta_{ij})$ appears instead of the usual factor of 2.

[26] *S. L. Simkhovich, A. S. Romanov, and L. I. Ionochkina, "Hydrodynamic Stability of a Generalized Nonlinear Visco-Plastic Fluid Under Plane Gradient Flow," translated from Inzhenemo-Fizicheskii Zhurnal, 46, No. 1, 60-64, 1983, Plenum Publishing Corp., 1984.*

$$\text{limit } K(T) \to 0,$$
$$T \to T_{\ell}(\rho)$$
$$\text{limit } \{f_s/(K(T)\Phi(\bar{F}))\} \to 0$$
$$T \to T_{\ell}(\rho)$$

Note that the above second limit is satisfied for any of the non-linear $\Phi(F \to \bar{F})$ functions proposed by Perzyna. Also, constitutive equation (7) provides for both rate-independent and rate-dependent material behavior. Hence, with an appropriate selection of material constants,[27] one should be able to approximate both instantaneous and non-instantaneous wave-propagation phenomena.[15]

Now that all the items contained within the energy equation have been defined, we can proceed with the development of the numerical solution scheme.

IV. DEVELOPMENT OF THE LINEAR MOMENTUM EQUATION FOR THE NUMERICAL SOLUTION

As previously discussed, we want to formulate the basic equations with respect to the FE approximation. This approximation involves discretizing the geometry (spatial variables) to obtain a set of time-dependent equations, and then solving this set using some other approximation.

A. Discretization of the Spatial Variables

In order to discretize the linear momentum equation (B.4) the previous strain-displacement and constitutive equations must be introduced for their corresponding terms. Furthermore, since the deviatoric behavior changes when $J>K(T)^2$, two different sets of equations must be developed; one for the elastic behavior and another for the fluid-type of behavior.

1. Elastic Behavior

The stress vectors $[\sigma_i]$ can be written as the following for i = 1, 2 and 3 respectively,

$$[\sigma_i] = [D_x][\varepsilon] - \begin{bmatrix} p \\ 0 \\ 0 \end{bmatrix} \tag{9}$$

---

[27] B. Bhushan and W. E. Jahsman, "Propagation of Weak Waves in Elastic-Plastic and Elastic-Viscoplastic Solids with Interfaces," Int. J. Solids Structures, 14, 39-51, 1978.

$$[\sigma_2] = [D_y][\varepsilon] - \begin{bmatrix} 0 \\ p \\ 0 \end{bmatrix} \tag{10}$$

$$[\sigma_3] = [D_z][\varepsilon] - \begin{bmatrix} 0 \\ 0 \\ p \end{bmatrix} \tag{11}$$

where $p = P(T,\rho) + 3K(T)\alpha(T)(T-T_D)$,

$$[D_x]^* = \begin{bmatrix} (\lambda+2G) & \lambda & \lambda & 0 & 0 & 0 \\ 0 & 0 & 0 & G & 0 & 0 \\ 0 & 0 & 0 & 0 & G & 0 \end{bmatrix},$$

$$[D_y]^* = \begin{bmatrix} 0 & 0 & 0 & G & 0 & 0 \\ \lambda & (\lambda+2G) & \lambda & 0 & 0 & 0 \\ 0 & 0 & 0 & 0 & 0 & G \end{bmatrix},$$

$$[D_z]^* = \begin{bmatrix} 0 & 0 & 0 & 0 & G & 0 \\ 0 & 0 & 0 & 0 & 0 & G \\ \lambda & \lambda & (\lambda+2G) & 0 & 0 & 0 \end{bmatrix},$$

$\lambda = \nu E/(1+\nu)(1-2\nu)$,

ν = Poisson's ratio,

E = Young's modulus,

$[\varepsilon] = [\varepsilon_{xx}\ \varepsilon_{yy}\ \varepsilon_{zz}\ \varepsilon_{xy}\ \varepsilon_{xz}\ \varepsilon_{yz}]^T$.

Note that the modulus can be a function of strain, i.e., non-linear, as long as there is no hysteresis upon unloading. Also, the bulk behavior $p_e \equiv K(T)(\sqrt{I_3}-1)$ has been included into the first matrix-product of equations (9) through (11).

Equation (1) can be written in matrix form as the following,

$$[\varepsilon] = [L][U] + [NLU]/2 \tag{12}$$

---

*For anisotropic elastic behavior, these matrices can be rewritten in terms of the elastic coefficients.

where $[L] = \begin{bmatrix} \partial/\partial x & 0 & 0 \\ 0 & \partial/\partial y & 0 \\ 0 & 0 & \partial/\partial z \\ \partial/\partial y & \partial/\partial x & 0 \\ \partial/\partial z & 0 & \partial/\partial x \\ 0 & \partial/\partial z & \partial/\partial y \end{bmatrix}$,

$$[NLU] = \begin{bmatrix} ([NLX][U])^T ([NLX][U]) \\ ([NLY][U])^T ([NLY][U]) \\ ([NLZ][U])^T ([NLZ][U]) \\ ([NLX][U])^T ([NLY][U]) \\ ([NLX][U])^T ([NLZ][U]) \\ ([NLY][U])^T ([NLZ][U]) \end{bmatrix},$$

$[NLX] = (\partial/\partial x)\ [I]$,

$[NLY] = (\partial/\partial y)\ [I]$,

$[NLZ] = (\partial/\partial z)\ [I]$,

$[I]$ = 3x3 Identity matrix,

$[U] = [u,v,w]^T$.

The last remaining step is to relate the displacements $[U]$ to the material velocities $[\bar{V}]$ using the kinematic relationship,

$$[U] = \int_{t_0}^{t} \{\bar{V}_1(x,y,z,\tau) + g_x(\tau)\}d\tau + u_0(x,y,z)$$

$$\int_{t_0}^{t} \{\bar{V}_2(x,y,z,\tau) + g_y(\tau)\}d\tau + v_0(x,y,z)$$

$$\int_{t_0}^{t} \{\bar{V}_3(x,y,z,\tau) + g_z(\tau)\}d\tau + w_0(x,y,z)$$

where $\bar{V}_i = \dot{u}, \dot{v}, \dot{w}$ respectively for $i = 1, 2, 3$ u_0, v_0 and w_0 represent the initial deformation at time t_0 and g_x, g_y and g_z represent the time-dependent motion associated with $R(t)$ and $\omega(t)$.

Using the above equations in the linear momentum equation (B.4), and rearranging all the non-linear terms to the right-hand side of the equation, yields the following non-linear integral-differential equation,

$$\int_V \left(\frac{\partial W}{\partial x}\ [D_x] + \frac{\partial W}{\partial y}\ [D_y] + \frac{\partial W}{\partial z}\ [D_z]\right)[L][U]dVol$$

$$= -\int_V \rho W\,[F_B]\,dVol - \int_V \rho W\,[\ddot{\bar{V}}]\,dVol + \int_S W\,[n][ST]\,dS$$

$$+ \int_V \left[\left(p\,\frac{\partial W}{\partial x}\right)\left(p\,\frac{\partial W}{\partial y}\right)\left(p\,\frac{\partial W}{\partial z}\right)\right]^T dVol + \int_{S_p(\tau)} W\,[\bar{V}]\rho[\bar{n}][\bar{V}]\,dS$$

$$- \sum_{K=1}^{11} [NL(K)]\,, \tag{14}$$

where $NL(1) = \int_V \frac{\partial W}{\partial x}\,[D_x][NLU]\,dVol,$

$NL(2) = \int_V \frac{\partial W}{\partial y}\,[D_y][NLU]\,dVol,$

$NL(3) = \int_V \frac{\partial W}{\partial z}\,[D_z][NLU]\,dVol,$

$NL(4) = \int_V \frac{\partial W}{\partial x}\,[\bar{A}][D_x][L][U]\,dVol,$

$NL(5) = \int_V \frac{\partial W}{\partial y}\,[\bar{A}][D_y][L][U]\,dVol,$

$NL(6) = \int_V \frac{\partial W}{\partial z}\,[\bar{A}][D_z][L][U]\,dVol,$

$NL(7) = -\int_V [\bar{A}]\left[\left(p\,\frac{\partial W}{\partial x}\right)\left(p\,\frac{\partial W}{\partial y}\right)\left(p\,\frac{\partial W}{\partial z}\right)\right]^T dVol,$

$NL(8) = -\int_S W[\bar{A}][n][T]\,dS,$

$NL(9) = \int_V \frac{\partial W}{\partial x}\,[\bar{A}][D_x][NLU]\,dVol,$

$NL(10) = \int_V \frac{\partial W}{\partial y}\,[\bar{A}][D_y][NLU]\,dVol,$

$NL(11) = \int_V \frac{\partial W}{\partial z}\,[\bar{A}][D_z][NLU]\,dVol.$

Note that, even when all the non-linear terms [NL] are identically zero, equation (14) is still implicitly non-linear because the pressure term p depends upon the density ρ, which in turn depends upon the deformations [U] through the relationship $\rho = \rho_o/\sqrt{I_3}$.

Based upon the above equation, the finite-element spatial discretization is developed in Appendix E-1. We can now consider the fluid-type of behavior.

2. Fluid-Type Behavior

For this case, previous equations (12) and (13) are still valid, and only the stress vectors $[\sigma_i]$ must be redefined. Furthermore, this definition depends upon whether the material is undergoing loading, unloading, or relaxation. For unloading, one forces the stress and strain to follow some function of the elastic slope (usually the so-called initial tangent-modulus E_o) up to some predefined set of stress and strains, after which the same constitutive equations are used. Therefore, this can be readily handled by the logic of the program and doesn't require a new set of equations. The relaxation behavior is predicted by solving a specific differential equation, and hence requires its own solution scheme. However, this scheme will not be developed for the current project. Therefore, only the specific set of equations associated with loading will be developed for the fluid-type of behavior.

The corresponding stress vectors $[\sigma_i]$ can be written as,

$$[\sigma_1] = [GX]([e] - [e^E]) + [ETAX]([\dot{e}] - [\dot{e}^E]) - \begin{bmatrix} (p+p_e) \\ 0 \\ 0 \end{bmatrix}, \tag{15}$$

$$[\sigma_2] = [GY]([e] - [e^E]) + [ETAY]([\dot{e}] - [\dot{e}^E]) - \begin{bmatrix} 0 \\ (p+p_e) \\ 0 \end{bmatrix}, \tag{16}$$

$$[\sigma_3] = [GZ]([e] - [e^E]) + [ETAZ]([\dot{e}] - [\dot{e}^E]) - \begin{bmatrix} 0 \\ 0 \\ (p+p_e) \end{bmatrix}, \tag{17}$$

where $[GX] = \begin{bmatrix} (2G_T) & 0 & 0 & 0 & 0 & 0 \\ 0 & 0 & 0 & G_T & 0 & 0 \\ 0 & 0 & 0 & 0 & G_T & 0 \end{bmatrix}$,

$$[GY] = \begin{bmatrix} 0 & 0 & 0 & G_T & 0 & 0 \\ 0 & (2G_T) & 0 & 0 & 0 & 0 \\ 0 & 0 & 0 & 0 & 0 & G_T \end{bmatrix},$$

$$[GZ] = \begin{bmatrix} 0 & 0 & 0 & 0 & G_T & 0 \\ 0 & 0 & 0 & 0 & 0 & G_T \\ 0 & 0 & (2G_T) & 0 & 0 & 0 \end{bmatrix},$$

$$[ETAX] = \begin{bmatrix} (2\eta_{eff}) & 0 & 0 & 0 & 0 & 0 \\ 0 & 0 & 0 & \eta_{eff} & 0 & 0 \\ 0 & 0 & 0 & 0 & \eta_{eff} & 0 \end{bmatrix},$$

$$[ETAY] = \begin{bmatrix} 0 & 0 & 0 & \eta_{eff} & 0 & 0 \\ 0 & (2\eta_{eff}) & 0 & 0 & 0 & 0 \\ 0 & 0 & 0 & 0 & 0 & \eta_{eff} \end{bmatrix},$$

$$[ETAZ] = \begin{bmatrix} 0 & 0 & 0 & 0 & \eta_{eff} & 0 \\ 0 & 0 & 0 & 0 & 0 & \eta_{eff} \\ 0 & 0 & (2\eta_{eff}) & 0 & 0 & 0 \end{bmatrix},$$

$$[\dot{e}] = [\dot{e}_{xx}, \dot{e}_{yy}, \dot{e}_{zz}, \dot{e}_{xy}, \dot{e}_{xz}, \dot{e}_{yz}]^T,$$

$$[e^E] = [e^E_{xx}, e^E_{yy}, e^E_{zz}, e^E_{xy}, e^E_{xz}, e^E_{yz}]^T,$$

and

$$[\dot{e}^E] = [\dot{e}^E_{xx}, \dot{e}^E_{yy}, \dot{e}^E_{zz}, \dot{e}^E_{xy}, \dot{e}^E_{xz}, \dot{e}^E_{yz}]^T.$$

Note that the individual terms e^E_{ij} and $\dot{e}^E_{ij}$ are determined from the previous definitions.

The deviatoric strain-rates $\dot{e}_{ij}$ are related to the strain-rates $\dot{\varepsilon}_{ij}$ via,

$$[\dot{e}] = [\dot{\varepsilon}] - [0\ 0\ 0\ \dot{f}\ \dot{f}\ \dot{f}]^T \tag{18}$$

where $f = 1/3(\sqrt{I_3}-1)$ and $\dot{f} = \partial f/\partial t$. The term $\sqrt{I_3}$ is the determinant of the matrix [A], and

$$[A] = \begin{bmatrix} (1+\partial u/\partial x) & 0 & 0 \\ 0 & (1+\partial v/\partial y) & 0 \\ 0 & 0 & (1+\partial w/\partial z) \end{bmatrix} + \begin{bmatrix} (\ 0\ ) & (\partial u/\partial y) & (\partial u/\partial z) \\ (\partial v/\partial x) & (\ 0\ ) & (\partial v/\partial z) \\ (\partial w/\partial x) & (\partial w/\partial y) & (\ 0\ ) \end{bmatrix} \tag{19}$$

The time derivative of this determinant can be written as the following determinant,

$$\frac{\partial}{\partial t}(\sqrt{I_3}) = \begin{vmatrix} \frac{\partial \dot{\bar{V}}_x}{\partial x} & \frac{\partial \dot{\bar{V}}_x}{\partial y} & \frac{\partial \dot{\bar{V}}_x}{\partial z} \\ \frac{\partial \bar{V}_y}{\partial x} & \frac{\partial \bar{V}_y}{\partial y} & \frac{\partial \bar{V}_y}{\partial z} \\ \frac{\partial \bar{V}_z}{\partial x} & \frac{\partial \bar{V}_z}{\partial y} & \frac{\partial \bar{V}_z}{\partial z} \end{vmatrix} , \tag{20}$$

where the order of differentiation was interchanged and equation (13) was used for [U].

The strain-rate matrix $[\dot{\varepsilon}]$ is given by the following equation,

$$[\dot{\varepsilon}] = [L][\bar{V}] + [\dot{NLU}] \tag{21}$$

where $[\dot{NLU}]_{6x1} = \Big[2(\frac{\partial u}{\partial x}\frac{\partial \dot{\bar{V}}_x}{\partial x} + \frac{\partial v}{\partial x}\frac{\partial \dot{\bar{V}}_y}{\partial x} + \frac{\partial w}{\partial x}\frac{\partial \dot{\bar{V}}_z}{\partial x})$

$2(\frac{\partial u}{\partial y}\frac{\partial \dot{\bar{V}}_x}{\partial y} + \frac{\partial v}{\partial y}\frac{\partial \dot{\bar{V}}_y}{\partial y} + \frac{\partial w}{\partial y}\frac{\partial \dot{\bar{V}}_z}{\partial y})$ $2(\frac{\partial u}{\partial z}\frac{\partial \dot{\bar{V}}_x}{\partial z} + \frac{\partial v}{\partial z}\frac{\partial \dot{\bar{V}}_y}{\partial z} + \frac{\partial w}{\partial z}\frac{\partial \dot{\bar{V}}_z}{\partial z})$

$(\frac{\partial \dot{\bar{V}}_x}{\partial x}\frac{\partial u}{\partial y} + \frac{\partial u}{\partial x}\frac{\partial \dot{\bar{V}}_x}{\partial y} + \frac{\partial \dot{\bar{V}}_y}{\partial x}\frac{\partial v}{\partial y} + \frac{\partial v}{\partial x}\frac{\partial \dot{\bar{V}}_y}{\partial y} + \frac{\partial \dot{\bar{V}}_z}{\partial x}\frac{\partial w}{\partial y} + \frac{\partial w}{\partial x}\frac{\partial \dot{\bar{V}}_z}{\partial y})$

$(\frac{\partial \dot{\bar{V}}_x}{\partial x}\frac{\partial u}{\partial z} + \frac{\partial u}{\partial x}\frac{\partial \dot{\bar{V}}_x}{\partial z} + \frac{\partial \dot{\bar{V}}_y}{\partial x}\frac{\partial v}{\partial z} + \frac{\partial v}{\partial x}\frac{\partial \dot{\bar{V}}_y}{\partial z} + \frac{\partial \dot{\bar{V}}_z}{\partial x}\frac{\partial w}{\partial z} + \frac{\partial w}{\partial x}\frac{\partial \dot{\bar{V}}_z}{\partial z})$

$(\frac{\partial \dot{\bar{V}}_x}{\partial y}\frac{\partial u}{\partial z} + \frac{\partial v}{\partial y}\frac{\partial \dot{\bar{V}}_x}{\partial z} + \frac{\partial \dot{\bar{V}}_y}{\partial y}\frac{\partial v}{\partial z} + \frac{\partial v}{\partial y}\frac{\partial \dot{\bar{V}}_y}{\partial z} + \frac{\partial \dot{\bar{V}}_z}{\partial y}\frac{\partial w}{\partial z} + \frac{\partial w}{\partial y}\frac{\partial \dot{\bar{V}}_z}{\partial z})\Big]^T .$

Now, using equations (15) through (21) in equation (B.4) and manipulating terms yields the following equation,

$$\int_V \Big(\frac{\partial W}{\partial x}[ETAX] + \frac{\partial W}{\partial y}[ETAY] + \frac{\partial W}{\partial z}[ETAZ]\Big)[L][\bar{V}]\, dVol$$

$$= -\int_V \rho W [F_B]\, dVol - \int_V \rho W [\dot{\bar{V}}]\, dVol + \int_S W [n][ST]\, dS$$

$$+ \int_V \Big[\Big((p+p_{\dot{e}})\frac{\partial W}{\partial x}\Big)\Big((p+p_e)\frac{\partial W}{\partial y}\Big)\Big((p+p_e)\frac{\partial W}{\partial z}\Big)\Big]^T dVol$$

$$+ \int_{S_{\dot{p}}(\tau)} W [\bar{V}]\rho [\bar{n}][\bar{V}]\, dS. - \int_V \Big(\frac{\partial W}{\partial x}[GX] + \frac{\partial W}{\partial y}[GY] \tag{22}$$

$$+ \frac{\partial W}{\partial z}[GZ])([L][U] - [H] - [e^E])\, dVol$$

$$+ \int_V (\frac{\partial W}{\partial x}[ETAX] + \frac{\partial W}{\partial y}[ETAY] + \frac{\partial W}{\partial z}[ETAZ])([\dot{e}^E] + [\dot{H}])\, dVol$$

$$= -\sum_{K=1}^{23} [NLF(K)],$$

where $NLF(1) = \int_V \frac{\partial W}{\partial x}[GX][NLU]\, dVol,$

$NLF(2) = \int_V \frac{\partial W}{\partial y}[GY][NLU]\, dVol,$

$NLF(3) = \int_V \frac{\partial W}{\partial z}[GZ][NLU]\, dVol,$

$NLF(4) = \int_V \frac{\partial W}{\partial x}[ETAX][NL\dot{U}]\, dVol,$

$NLF(5) = \int_V \frac{\partial W}{\partial y}[ETAY][NL\dot{U}]\, dVol,$

$NLF(6) = \int_V \frac{\partial W}{\partial z}[ETAZ][NL\dot{U}]\, dVol,$

$NLF(7) = \int_V \frac{\partial W}{\partial x}[\bar{A}][GX]([L][U] - [H] - [e^E])\, dVol,$

$NLF(8) = \int_V \frac{\partial W}{\partial y}[\bar{A}][GY]([L][U] - [H] - [e^E])\, dVol,$

$NLF(9) = \int_V \frac{\partial W}{\partial z}[\bar{A}][GZ]([L][U] - [H] - [e^E])\, dVol,$

$NLF(10) = -\int_V [\bar{A}][((p+p_e)\frac{\partial W}{\partial x})((p+p_e)\frac{\partial W}{\partial y})((p+p_e)\frac{\partial W}{\partial z})]^T\, dVol,$

$NLF(11) = -\int_S [\bar{A}]\, W\, [n][ST]\, dS,$

$NLF(12) = \int_V \frac{\partial W}{\partial x}[\bar{A}][GX][NLU]\, dVol,$

$NLF(13) = \int_V \frac{\partial W}{\partial y}[\bar{A}][GY][NLU]\, dVol,$

$NLF(14) = \int_V \frac{\partial W}{\partial z}[\bar{A}][GZ][NLU]\, dVol,$

$$NLF(15) = \int_V \frac{\partial W}{\partial x} [\bar{A}][ETAX]([L][\bar{V}] - [\dot{e}^E])\, dVol,$$

$$NLF(16) = \int_V \frac{\partial W}{\partial y} [\bar{A}][ETAY]([L][\bar{V}] - [\dot{e}^E])\, dVol,$$

$$NLF(17) = \int_V \frac{\partial W}{\partial z} [\bar{A}][ETAZ]([L][\bar{V}] - [\dot{e}^E])\, dVol,$$

$$NLF(18) = -\int_V \frac{\partial W}{\partial x} [\bar{A}][ETAX][\dot{H}]\, dVol,$$

$$NLF(19) = -\int_V \frac{\partial W}{\partial y} [\bar{A}][ETAY][\dot{H}]\, dVol,$$

$$NLF(20) = -\int_V \frac{\partial W}{\partial z} [\bar{A}][ETAZ][\dot{H}]\, dVol,$$

$$NLF(21) = \int_V \frac{\partial W}{\partial x} [\bar{A}][ETAX][NL\dot{U}]\, dVol,$$

$$NLF(22) = \int_V \frac{\partial W}{\partial y} [\bar{A}][ETAY][NL\dot{U}]\, dVol,$$

$$NLF(23) = \int_V \frac{\partial W}{\partial z} [\bar{A}][ETAZ][NL\dot{U}]\, dVol,$$

$$H = [0\ 0\ 0\ f\ f\ f]^T,$$

and

$$\dot{H} = [0\ 0\ 0\ \dot{f}\ \dot{f}\ \dot{f}]^T.$$

It should be noted that, even if all the NLF matrices were zero, equation (22) is still a non-linear differential equation since the effective viscosity depends upon the unknowns $[\bar{V}]$ and T. Equation (19) is spatially discretized in Appendix E-2.

B. Discretization of the Temporal Variable

The equations given in Appendix E represent a set of non-linear, first order, differential equations (actually an integral-differential equation for the elastic behavior) for the unknown material velocities $[\bar{V}]$. Hence, an additional approximation must be introduced in order to obtain a solution. Numerous FE programs use finite-differences to obtain a discretization of the temporal variable, with the explicit forward-differences being the most common technique. A few programs use the implicit Crank-Nicolson (central difference) scheme, which has second-order accuracy with respect to truncation errors in a linear problem. Baker[4] uses the Method of Weighted Residuals (the FE method) and finds the approximate solutions to be as good,

or better than, the solutions from the Crank-Nicolson method. A similar observation was made in reference 28 based upon simple first and second order equations. Therefore, the author decided to use the FE method for the temporal discretization.

Depending upon the choice of the time-weighting function, a wide variety of time-marching equations can be obtained, with some equations yielding better approximations than others (see references 8 and 27). A variety of final equations are presented in Appendix F, and during the second year of research the author will attempt to ascertain which equations yield the best approximation.

V. DEVELOPMENT OF THE ENERGY EQUATION FOR THE NUMERICAL SOLUTION

The energy equation (D.4) must be rewritten in terms of the unknowns $[\overline{V}]$ and T by using the EOS, strain-displacement, and constitutive equations. Furthermore, the equation takes different forms depending upon both the thermodynamic phase and the deviatoric stress behavior, i.e., whether $J \leq K(T)^2$, or $> K(T)^2$.

Hence, in order to spatially discretize equation (D.4), several new terms must be explicitly developed. The first term involves the time derivative of the thermal part of the EOS. This part can be written as $B(T) + B_1(T,\sqrt{I}_3)\ T + B_2(T,\sqrt{I}_3)\ T^2$, where the B coefficients depend upon the the thermodynamic phase of the material. Therefore, the time derivative becomes,

$$\frac{\partial}{\partial t}(\text{thermal part of EOS}) = \frac{dB}{dT}\frac{\partial T}{\partial t} + \frac{\partial B_1}{\partial T}\frac{\partial T}{\partial t}\,T$$

$$+ \frac{\partial B_1}{\partial \sqrt{I}_3}\frac{\partial \sqrt{I}_3}{\partial t}\,T + B_1\frac{\partial T}{\partial t} + \frac{\partial B_2}{\partial T}\frac{\partial T}{\partial t}\,T^2 \qquad (23)$$

$$+ \frac{\partial B_2}{\partial \sqrt{I}_3}\frac{\partial \sqrt{I}_3}{\partial t}\,T^2 + 2B_2\,T\frac{\partial T}{\partial t},$$

which has the general form of $\beta_1(T) + \beta_2(T)\,\dot{T}$.

---

[36] O.C. Zienkiewicz and K. Morgan, *FINITE ELEMENTS AND APPROXIMATION*, Chapter 7, John Wiley and Sons, Inc., 1983.

Another new term is the product $[\dot{\varepsilon}]^T [\sigma_{ij}]$ of strain-rate and stress. However, the strain-rate is discretized in Appendix E and this product can be readily evaluated by using a slightly different form of equations (9) - (11) and equations (15) - (17). Therefore, using equation (23) and the same spatial and temporal discretizations as used in the linear momentum equation, the energy equation can be fully discretized and this development is presented in Appendix G.

VI SUMMARY

In order to develop a predictive 2-D model for penetration problems, a self-consistent set of equations was developed. This set of equations includes the concept of polymorphic and thermodynamic phase changes, and uses a corrected BRL version of the GRAY three-phase equation-of-state. Since the critical temperatures and pressures have already been established by the BRL for 18 different metals, existing data and FORTRAN coding can be incorporated into the new model. The polymorphic changes are incorporated via existing Hugoniot data which exhibit volumetric discontinuity at various pressures.

In addition to the equations-of-state, the new model also considers a constitutive equation involving both the scalar pressure (which is dependent upon volume change and temperature) and a deviatoric stress. This deviatoric stress contains both strain and strain-rate contributions with temperature dependent material properties. Furthermore, this deviatoric stress maps continuously between the solid and fluid (liquid and vapor) states of the material. Also, the deviatoric stress depends upon the entire history of the velocities, and hence the model could be applied to temperature-dependent viscoelastic materials such as plastics.

Because of the thermodynamic phase-changes, the conservation of mass equation is written in a global fashion to keep track of the mass contained with the solid-liquid-vapor phases. Furthermore, mass can be convected out of one phase into another and the corresponding momentum and energy fluxes are considered in the conservation equations.

Since large extensions and rotations of material can readily occur during a penetration process, the new model uses the strain-displacement relationships which include the second-order terms. Also, the finite deformation definition is used to represent volumetric changes within a material. Lastly, to account for a possible reorientation of the stresses during a time-step, the nonlinear forms of the linear and angular momentum equations are used.

Since temperature is one of the essential unknowns, the energy equation is introduced along with the possibility of conductive, convective and radiation heat fluxes, internal heat generation due to latent heat and chemical reactions, internal kinetic and stored strain energies, work of inertial forces and applied surface tractions, and internal irreversible work. Note that generalized inertial forces are included in all of the conservation equations so that problems involving bodies with translational acceleration, and rotational velocities and accelerations, can be considered for analysis.

The above resulting set of differential and integral-differential equations are extremely nonlinear and are coupled together. Even when applied to the idealized problem of a stretching, one-dimensional shaped-charge jet, the resulting set of equations cannot be directly integrated. Hence, the author introduced an approximation by discretizing the equations in both time and space. This discretization involved the method of weighted residuals using piecewise continuous weighting and trial functions. This converts

the original nonlinear differential equations into a set of nonlinear algebraic equations which must be evaluated at each time-step. This incremental solution involves algebraic recursion relationships which depend upon the assumed weighting and trial functions. A wide variety of recursion relationships were derived and are presented in the appendices.

The beauty of this newly developed set of equations is that almost all nonlinearities appear as separate entities within the equations. Hence, the various nonlinear contributions may be successively "turned on" by either the user or some sort of computer logic. Also, the user can specify regions with different nonlinear contributions which the computer logic can bring "in and out" for the analysis of the different regions. Furthermore, one, two, and three dimensional contributions have been individually identified along with their contribution to the order of the matrices. Therefore, the 2-D formulation can be readily updated to 3-D type of problems once the appropriate functions and matrices are modified.

The last aspect of the new model is the "creation and annihilation" concept where the original geometric configuration is subdivided into a set of super-elements, each of which are assumed to be quasi-independent. Each super-element can have its own degree of nonlinearity, with the vast majority of the super-elements being governed by the fully linearized momentum and energy equations. Furthermore, each super-element has its own set of discretized equations which must be solved in an incremental (and possibly iteratively) fashion subject to its boundary conditions. However, many of these boundary conditions correspond to the common interface between various super-elements. At these common interfaces, the velocities, tractions, temperatures and heat-flux must match between the interconnected super-elements. Therefore, these interface conditions must be matched via an iterative fashion at certain time-steps during the time interval. However, it appears that this iterative C and A process will yield an approximate solution faster than current FE or hydrodynamic approaches.

ACKNOWLEDGEMENTS

The author wishes to acknowledge the non-government funded, quarter-time release which was provided by the College of Engineering of Villanova University. This additional release-time enabled the author to devote considerably more effort towards this research project and contributed to its success. Also, the author wishes to thank three graduate students, Mr. M. Kangutkar, Mr. K. Raichur, and Mr. S. Tipparaju, who checked the calculus and algebra in the derivation of many of the equations contained within the appendices.

LIST OF REFERENCES

1. J. T. Oden and G. F. Carey, FINITE ELEMENTS: SPECIAL PROBLEMS IN SOLID MECHANICS, Volume V of the Texas Finite Element Series, Prentice-Hall Inc., New Jersey, 1984.

2. O. C. Zienkiewicz and P. N. Godbole, "Flow of Plastic and Visco-Plastic Solids with Special Reference to Extrusion and Forming Processes," Int. J. Num. Meth. Engr., 8, 3-16, 1974.

3. O. C. Zienkiewicz and C. J. Parekh, "Transient Field Problems: Two-Dimensional and Three-Dimensional Analysis by Isoparametric Finite Elements," Int. J. of Numerical Methods Engr., 2, 61-71, 1970.

4. A. J. Baker, FINITE ELEMENT COMPUTATIONAL FLUID MECHANICS, Hemisphere Publishing Corp., New York, 1983.

5. L. H. VanVlack, MATERIALS FOR ENGINEERING, Chapters 5 and 6, Addison-Wesley Publishing Co., Reading, Mass., 1982.

6. Ibid, Chapters 2 and 11.

7. O. C. Zienkiewicz, THE FINITE ELEMENT METHOD IN ENGINEERING SCIENCE, Chapter 9, McGraw-Hill, London, 1971.

8. L. J. Segerlind, APPLIED FINITE ELEMENT ANALYSIS, Chapters 14-16, John Wiley & Sons, Inc., New York, 1976.

9. G. F. Carey and J. T. Oden, FINITE ELEMENTS: A SECOND COURSE, Volume II in the Texas Finite Element Series, Chapters 1 and 2, Prentice-Hall, Inc., New Jersey, 1983.

10. V. V. Novozhilov, THEORY OF ELASTICITY, pp 18-88, translation of Russian book TEORIYA UPRUGOSTI (1958), Israel Program for Scientific Translation, OTS61-11401, Jerusalem, 1961.

11. S. K. Godunov, A. F. Demchuk, N. S. Kozin and V. I. Mali, "Interpolation Formulas for Maxwell Viscosity of Certain Metals as a Function of Shear-Strain Intensity and Temperature," translated from Zhurnal Prikladnoi Prikladnoi Mekhaniki i Teknicheskoi Fiziki (1974), Plenum Publishing Corp., 1976.

12. G. E. Duvall and D. P. Dandekar, "Theory of Equations of State: Elastic-Plastic Effects II," USA Ballistic Research Laboratories Contract Report No. 106, May, 1973.

13. H. B. Callen, THERMODYNAMICS, Appendices D and E, John Wiley and Sons, Inc., New York, 4th Printing, 1963.

14. F. H. Harlow and A. A. Amsden, FLUID MECHANICS, A LASL MONOGRAPH, Los Alamos Scientific Laboratory, Report No. LA-4700, June, 1971.

15. N. Cristescu, DYNAMIC PLASTICITY, Chaps 8, 10, North-Holland Publishing Co., John Wiley and Sons distributors, 1967.

16. J. de Beaumont and J. Leygonie, "Vaporization of Uranium after Shock Loading," Proceedings of the Fifth Symposium (International) on Detonation, Pasadena, California, ACR-184-, pp 547-558, August 18-21, 1970.

17. J. H. Tillotson, "Metal Equations of State for Hypervelocity Impact," General Atomic Report GA-3216, July 1962.

18. E. B. Royce, "GRAY, A Three-Phase Equation of State for Metals," Lawrence Livermore Laboratory, UCRL-51121, September 1971.

19. J. F. Lacetera, "BRLGRAY: The Ballistic Research Laboratory Version of the GRAY Equation of State," U.S. ARRADCOM Ballistic Research Laboratory Technical Report ARBRL-TR-02258, August 1980.

20. C. Truesdell, "Elasticity and Fluid Dynamics," J. Rational Mechanics and Analysis, 1, 126-262, 1952, and Vol 2, 593-611, 1953.

21. Walter Noll, "On the Continuity of the Solid and Fluid States," J. Rational Mechanics and Analysis, 4, 3-81, 1955.

22. Walter Noll, "A Mathematical Theory of the Mechanical Behavior of Continuous Media," Archives Rational Mech. Analysis, 2, 198-226, 1958.

23. Proceedings of the International Conference on Constitutive Laws for Engineering Materials: Theory and Application, Tucson, Arizona, January 1983.

24. P. Perzyna, "The Constitutive Equation for Rate Sensitive Plastic Materials," Quarterly Appl. Math., XX, No. 4, 321-322, 1963.

25. O. C. Zienkiewicz, P. C. Jain and E. Onate, "Flow of Solids During Forming and Extrusion: Some Aspects of Numerical Solutions," Int. J. Solids Structures, 14, 15-38, 1978.

26. S. L. Simkhovich, A. S. Romanov, and L. I. Ionochkina, "Hydrodynamic Stability of a Generalized Nonlinear Visco-Plastic Fluid Under Plane Gradient Flow," translated from Inzhenemo-Fizicheskii Zhurnl, 45, No. 1, 60-64, 1983, Plenum Publishing Corp., 1984.

27. B. Bhushan and W. E. Jahsman, "Propagation of Weak Waves in Elastic-Plastic and Elastic-Viscoplastic Solids with Interfaces," Int. J. Solids Structures, 14, 39-51, 1978.

28. O. C. Zienkiewicz and K. Morgan, FINITE ELEMENTS AND APPROXIMATION, Chapter 7, John Wiley and Sons, Inc., 1983.

29. B. A. Boley and J. H. Weiner, THEORY OF THERMAL STRESSES, Chapter 2, John Wiley and Sons, Inc., 1960.

30. N. M. Newmark, "A Method for Computation of Structural Dynamics," Proc. Am. Soc. Civil Eng., 85, EMS, pp 67-94, 1959.

LIST OF SYMBOLS

$C_v(T)$ = coefficient of specific heat at constant volume,

dVol = elemental volume,

E = Young's modulus

$E(T,\rho)$ = internal energy per unit mass,

e_{ij} = ij^{th} component of the deviatoric strain-tensor,

F_B = inertial body-force,

$f = 1/3(\sqrt{I_3}-1)$,

f_e = volume fraction of reversible "plastic" work,

f_f = volume fraction of fluid material,

f_p = volume fraction of irreversible "plastic" work,

f_s = volume fraction of solid material,

G = shear modulus,

G_T = strain-hardening shear modulus,

I_3 = third strain-invariant of the ε strain,

$I_{\dot{e}}^{(2)} = \frac{1}{2}\,\dot{e}_{ij}\,\dot{e}_{ij}$,

$I_e^{(2)} = \frac{1}{2}\,e_{ij}\,e_{ij}$,

$I_s^{(2)} = \frac{1}{2}\,S_{ij}\,S_{ij}$,

K = yield stress in simple shear,

$K_{\ell\ell}$ = thermal conductivity in the $\ell\ell^{th}$ principal material direction,

$\hat{n}$ = outward unit-vector normal to a surface,

$P(T,\rho)$ = Equation-of-state (EOS) pressure,

$P_H(\rho)$ = Hugoniot pressure,

$p = P(T,\rho) + 3\kappa(T)\alpha(T)(T-T_D)$,

$p_e = \kappa(T)(\sqrt{I_3}-1)$

Q = heat source or sink per unit mass,

$\underset{\sim}{q}$ = specified heat-flux across a surface,

$\hat{R}$ = global position vector with respect to inertial coordinates,

R' = Universal Gas Constant/Atomic weight,

$\hat{r}$ = Local position vector with respect to an attached rectangular cartesian coordinate system,

$S_p(t)$ = surface separating two different material phases at time t,

S_{ij} = ij^{th} component of the "extra" or deviatoric stress-tensor,

T = temperature ^oK,

T_D = Debye temperature,

$T_\ell(\rho)$ = liquidus temperature,

$T_s(\rho)$ = solidus temperature,

t = time,

t_o = initial time,

U_s = shock velocity,

U_p = particle velocity,

$V(j)$ = volume of the j^{th} sub-domain at the start of a time-step,

$\overline{V}_i$ = material velocity in the i^{th} direction,

W = Spatial Weighting function,

W_A = Atomic weight,

WT = temporal weighting function,

$\alpha(T)$ = unidirectional coefficient of thermal expansion,

$\Delta T = T_\ell(\rho) - T_s(\rho)$,

Δt = time-step size,

ε_{ij} = ij^{th} component of the strain tensor,

η_{eff} = effective material-viscosity,

$\kappa(T)$ = elastic bulk-modulus coefficient,

λ = Lame's constant,

ρ = mass density,

σ_{ij} = ij^{th} component of the stress tensor,

τ = time-variable,

$\bar{\tau}$ = dimensionless time-variable,

$\Phi(F)$ = Perzyna's plasticity function,

Ω_i = rotational velocity about the i^{th} axis of a coordinate system,

Ω_i = angular acceleration about the i^{th} axis,

ω = rotational angle,

$[\ldots]_{nxm}$ = a matrix with n-rows and m-columns.

APPENDIX A

CONSERVATION OF MASS EQUATION

Integrating over the volume V of any particular phase, and considering possible phase-boundaries S_p, the mass conservation equation can be written as,

$$\int_{V(t_o)} \rho(t_o)\,dVol - \int_{V(t)} \rho(t)\,dVol = \int_{t_o}^{t} \left(\int_{S_p(\tau)} \rho \bar{V}\cdot\hat{n}\,ds \right) d\tau \qquad (A.1)$$

where ρ = mass density,
$dVol$ = elemental volume,
$\hat{n}$ = outward unit vector normal to the phase-boundary,
$\bar{V}$ = material velocity across the phase-boundary.

Note that the term inside the parentheses on the right hand side of the equation (A.1) is the instantaneous mass-flux across the phase-boundary and will be denoted as $\dot{M}_p(\tau)$. The total mass of the system is conserved and can be written in the global sense as

$$M_o = \int_{V_s(t)} \rho_s\,dVol + \int_{V_\ell(t)} \rho_\ell\,dVol + \int_{V_v(t)} \rho_v\,dVol \qquad (A.2)$$

where $V_s(t)$ = volume of solid at time t,

$V_\ell(t)$ = volume of liquid at time t,

$V_v(t)$ = volume of vapor at time t,

ρ_s = solid density, and

ρ_ℓ = liquid density,

ρ_v = vapor density.

APPENDIX B

CONSERVATION OF LINEAR MOMENTUM EQUATIONS

Based upon the assumptions discussed in the text, Novozhilov's linear momentum equations can be written in the following elemental form,

$$\nabla \cdot ([A_i]\ [\sigma_1]\hat{i} + [A_i]\ [\sigma_2]\hat{j} + [A_i]\ [\sigma_3]\hat{k}) \tag{B.1}$$

$$- \rho F_{Bi} = \rho \frac{\partial \bar{V}_i}{\partial t} + \left(V_i \frac{\partial \rho}{\partial t}\right)^* \quad i=1,2,3$$

where $\nabla = \frac{\partial}{\partial x}\hat{i} + \frac{\partial}{\partial y}\hat{j} + \frac{\partial}{\partial z}\hat{k}$,

$[A_i]$ = row matrix associated with the ith row of $[A]$,

$$[A] = \begin{bmatrix} (1+\partial u/\partial x) & (\partial u/\partial y) & (\partial u/\partial z) \\ (\partial v/\partial x) & (1+\partial v/\partial y) & (\partial v/\partial z) \\ (\partial w/\partial x) & (\partial w/\partial y) & (1+\partial w/\partial z) \end{bmatrix}$$

$[\sigma_i]$ = column matrix associated with ith column of the stress matrix $[\sigma]$,

$$[\sigma] = \begin{bmatrix} \sigma_{xx} & \sigma_{yx} & \sigma_{zx} \\ \sigma_{xy} & \sigma_{yy} & \sigma_{zy} \\ \sigma_{xz} & \sigma_{yz} & \sigma_{zz} \end{bmatrix},$$

u, v, w, = components of the displacement vector,

$\dot{R}_i$ = time derivative of the ith component of the global position-vector $\hat{R}$,

F_{Bi} = ith component of the inertial body-forces per unit mass,

σ_{ij} = ijth component of stress,

$\bar{V}_i$ = $\dot{u}$, $\dot{v}$ or $\dot{w}$ for i = 1, 2, 3 respectively.

Applying the method of weighted residuals, equation (B.1) is multiplied by some weighting function W(x,y,z), and the resulting equation is integrated over the entire body, i.e.,

$$\int_{V(t)} W \nabla \cdot ([A_i]\ [\sigma_1]\hat{i} + [A_i]\ [\sigma_2]\hat{j} + [A_i]\ [\sigma_3]\hat{k}) dVol - \int_{V(t)} \rho W F_{Bi}\ dVol \tag{B.2}$$

$$= \int_{V(t)} \rho W \frac{\partial \bar{V}_i}{\partial t} dVol - \int_{S_p(t)} W \bar{V}_i (\rho \bar{V}_i n_i) dS,$$

---

*Term added by the author to represent possible mass-change within the elemental volume.

where n_i is the direction cosine for the ith spatial direction. The last term represents the linear momentum flux across the phase boundary, and corresponds to the $(\bar{V}_i \partial\rho/dt)$ term in equation (B.1) coupled with the conservation-of-mass equation in equation (A.1).

The first term in equation (B.2) has the form (f div u) which, from calculus, equals (div (fu) - u·gradf), and the volume integral over div(fu) can be replaced by a surface integral using the Gauss divergence theorem. Using these facts yields the following weak-form of the weighted residuals,

$$
\begin{aligned}
&-\int_{V(t)}([A_i]\ [\sigma_1]\hat{i} + [A_i]\ [\sigma_2]\hat{j} + [A_i]\ [\sigma_3]\hat{k})\cdot\nabla W dVol \\
&+\int_{S(t)} W([A_i]\ [\sigma_1]\hat{i} + [A_i]\ [\sigma_2]\hat{j} + [A_i]\ [\sigma_3]\hat{k})\cdot\hat{n}dS \qquad \text{(B.3)} \\
&-\int_{V(t)}\rho W F_{Bi} dVol = \int_{V(t)}\rho W \frac{\partial \bar{V}_i}{\partial t} dVol \quad - \quad \int_{S_p(t)} W\,\bar{V}_i(\rho \bar{V}_i n_i)dS \quad ,
\end{aligned}
$$

where S represents the surfaces where surface tractions t_{ij} are specified.

The above three equations can be written as a single matrix equation of the following form,

$$
\begin{aligned}
&-\int_{V(t)}\left(\frac{\partial W}{\partial x}[\sigma_1] + \frac{\partial W}{\partial y}[\sigma_2] + \frac{\partial W}{\partial z}[\sigma_3]\right)dVol = \int_{V(t)}\rho W[F_B]dVol \\
&+\int_{V(t)}\rho W \frac{\partial}{\partial t}[\bar{V}]dVol \quad - \int_{S(t)} W([n]\,[ST] + [\bar{A}]\,[n]\,[ST])dS \qquad \text{(B.4)} \\
&+\int_{V(t)}\left(\frac{\partial W}{\partial x}[\bar{A}][\sigma_1] + \frac{\partial W}{\partial y}[\bar{A}][\sigma_2] + \frac{\partial W}{\partial z}[\bar{A}]\,[\sigma_3]\right)dVol \\
&- \int_{S_p(t)} W\rho\,[\bar{V}]\,[\bar{n}]\,[\bar{V}]dS
\end{aligned}
$$

where $[n] = \begin{bmatrix} n_x & 0 & 0 \\ 0 & n_y & 0 \\ 0 & 0 & n_z \end{bmatrix}$, $[\bar{n}] = [n_x n_y n_z]$,

$$[ST] = \begin{bmatrix} (t_{xx} + t_{yx} + t_{zx}) \\ (t_{yx} + t_{yy} + t_{yz}) \\ (t_{zx} + t_{yz} + t_{zz}) \end{bmatrix},$$

$$[\bar{A}] = \begin{bmatrix} (\partial u/\partial x)(\partial u/\partial y)(\partial u/\partial z) \\ (\partial v/\partial x)(\partial v/\partial y)(\partial v/\partial z) \\ (\partial w/\partial x)(\partial w/\partial y)(\partial w/\partial z) \end{bmatrix},$$

$$F_{Bi} = (\dot{\Omega}_j r_k - \dot{\Omega}_k r_j) + 2(\Omega_j \bar{V}_k - \Omega_k \bar{V}_j) + \ddot{R}_x$$

$$\pm (\Omega_j r_j + \Omega_k r_k) \Omega_i - (\Omega_j^2 + \Omega_k^2) r_i,$$

Ω_i = rotational velocity of local material coordinate system about ith axis of the local fixed coordinate system,

$\dot{\Omega}_i$ = angular acceleration about the ith axis,

r_i = ith component (r_x, r_y or r_z) of the local position vector $\hat{r}$.

Note that the $[\bar{A}]$ term corresponds to finite rotation of the infinitesimal volume, and is usually assumed as zero. The first term in the body-force F_B expression is usually called the "linear-acceleration" body-force, the second term is the "coriolis" body-force, the third term is the classical d'Alembert body-force, and the last two terms are associated with the "centripetal" body-force.

APPENDIX C

CONSERVATION OF ANGULAR MOMENTUM EQUATIONS

The elemental form of the angular momentum equation is developed by taking the cross product between the position vector R and the stress vectors, and equating this to the time derivative of $(R\times(m\hat{v}))$. Multiplying these products by the weighting function, using the fact that $\hat{R}\times\hat{v}\equiv 0$, $R=R+r$, and, R is independent of dVol, integration over the volume yields three equations of the following form,

$$\int_{V(t)} W\Big\{r_j\nabla\cdot([A_k]\,[\sigma_1]\hat{i}+[A_k]\,[\sigma_2]\hat{j}+[A_k]\,[\sigma_3]\hat{k})$$

$$-r_k\nabla\cdot([A_j]\,[\sigma_1]\hat{i}+[A_j]\,[\sigma_2]\hat{j}+[A_j]\,[\sigma_3]\hat{k})\Big\}\,dVol \qquad (C.1)$$

$$\int_{V(t)}\rho W(r_j F_{Bk}-r_k F_{Bj})\,dVol = \int_{V(t)} W\rho\left(r_j\frac{\partial V_k}{\partial t}-r_k\frac{\partial V_j}{\partial t}\right)dVol$$

minus the Weighted Angular Momentum Flux across phase boundaries,* plus one vector equation of the form $\hat{R}\times$ left-hand-side minus right-hand-side of equation (B.4). Therefore, when the linear momentum equation (B.4) is satisfied, this vector equation is identically equal to zero.

Equation (C.1) can be rewritten using the calculus identity involving $f\,\mathrm{div}u = \mathrm{div}(fu)-u\cdot\mathrm{grad}f$, with $f\equiv Wr_i$, and then using the Gauss divergence theorem to yield,

$$\Big\{-\int_{V(t)}([A_k]\,[\sigma_1]\hat{i}+[A_k]\,[\sigma_2]\hat{j}+[A_k]\,[\sigma_3]\hat{k})\cdot\nabla(r_j W)\,dVol$$

$$+\int_{S(t)} r_j W([A_k]\,[\sigma_1]\hat{i}+[A_k]\,[\sigma_2]\hat{j}+[A_k]\,[\sigma_3]\hat{k})\cdot\hat{n}\,dS$$

$$-\int_{V(t)} r_j\rho W F_{Bk}\,dVol - \int_{V(t)} r_j W\rho\frac{\partial\bar{V}_k}{\partial t}\,dVol\Big\} \qquad (C.2)$$

$$-\Big\{-\int_{V(t)}([A_j]\,[\sigma_1]\hat{i}+[A_j]\,[\sigma_2]\hat{j}+[A_j]\,[\sigma_3]\hat{k})\cdot\nabla(r_k W)\,dVol$$

$$+\int_{S(t)} r_k W([A_j]\,[\sigma_1]\hat{i}+[A_j]\,[\sigma_2]\hat{j}+[A_j]\,[\sigma_3]\hat{k})\cdot\hat{n}\,dS$$

$$-\int_{V(t)} r_k\rho W F_{Bj}\,dVol - \int_{V(t)} r_k W\rho\frac{\partial\bar{V}_j}{\partial t}\,dVol\Big\} \quad +\text{ith Component of Weighted Angular Momentum flux} = 0$$

*Note that this quantity corresponds to the weighted volume-integral of the $\{r\times(\dot{R}+\bar{V}+\dot{r}\times r)\dot{M}_p\}$ terms.

Comparison of the terms within each bracket of equation (C.2) with the linear momentum equations (B.3) shows that each term corresponds to a linear momentum equation whose integrand is multiplied by a component of the position vector. Obviously, if the linear momentum equation is satisfied at all points within the body, then equations of the form of equation (C.2) are also satisfied. However, the linear momentum equations are only satisfied in an integral sense, and therefore the angular momentum equations will be automatically satisfied <u>only</u> for certain special situations:

a. the linear momentum integrand is independent of the position component r_i

b. the linear momentum integrand is symmetrical with respect to the position component r_i.

APPENDIX D

CONSERVATION OF ENERGY EQUATION

The conservation of energy is usually stated as the time-rate of change of the internal energy being equal to the sum of the energy flux into the system plus the time-rate of change of the heat added to the system and the work done on the system. Based upon the assumptions mentioned in the text, the components of the energy equation for an elemental mass can be written as

$$\frac{\partial}{\partial t}(\text{heat added}) = \rho\dot{Q}d\text{Vol} - (k_{xx}\frac{\partial T}{\partial y}n_x + k_{yy}\frac{\partial T}{\partial y}n_y + k_{zz}\frac{\partial T}{\partial z}n_z)dS + f_p\,[\dot{\varepsilon}]^T[\sigma_{ij}]d\text{Vol} \tag{D.1}$$

$$\frac{\partial}{\partial t}(\text{work done}) = [ST]^T\,[n]^T\,([I] + [\bar{A}]^T)\left\{[\dot{R}]+[\bar{V}]+[\hat{\Omega}x\hat{r}]\right\}dS \tag{D.2}$$

$$\frac{\partial}{\partial t}(\text{internal energy}) = \left\{\frac{\partial}{\partial t}(\text{thermal energy}) + f_e[\dot{\varepsilon}]^T\,[\sigma_{ij}]\right. \tag{D.3}$$

$$\left. + \frac{\partial}{\partial t}\left(\frac{\rho}{2}\,([\dot{R}]^T+[\bar{V}]^T+[\hat{\Omega}x\hat{r}]^T)\;\;([\dot{R}]+[\bar{V}]+[\hat{\Omega}x\hat{r}])\right)\right\} d\text{Vol}\,.$$

In equation (D.1), the $\dot{Q}$ term is positive for an exothermic heat source per unit mass, Fourier's Law is assumed to hold for conductive heat flow, T represents the absolute temperature, $\dot{\varepsilon}_{ij}$ is the time-rate of change of the ijth component of the strain, σ_{ij} is the ijth component of the stress, and f_p is the volume fraction ($0 \leq f_p \leq 1$) for non-elastic deformations. In equation (D.2), $\hat{\Omega}$ is the rotational velocity-vector ($\Omega_1\hat{i}+\Omega_2\hat{j}+\Omega_3\hat{k}$), and in equation (D.3), f_e is the volume fraction ($f_e+f_p=1$) for elastic deformations.

Substituting the above definitions into the conservation of energy equation, multiplying by a weighting function W, and integrating over the entire spatial domain, yields the following equation,

$$\int_{V(t)} W\left\{\rho\frac{\partial}{\partial t}(\text{thermal part of EOS}) + f_e[\dot{\varepsilon}]^T\,[\sigma_{ij}]\right\}d\text{Vol}$$

$$+[\dot{R}]^T * \text{weighted linear momentum Eq} + [\hat{\Omega}]^T * \text{weighted angular momentum Eq}$$

$$+\int_{V(t)}[\bar{V}]^T\left\{\frac{\partial W[\sigma_1]}{\partial x} + \frac{\partial W[\sigma_2]}{\partial y} + \frac{\partial W[\sigma_3]}{\partial z} + \rho W([F_B] + [\dot{\bar{V}}]) + \frac{\partial W[\bar{A}][\sigma_1]}{\partial x} + \frac{\partial W[\bar{A}][\sigma_2]}{\partial y}\right. \tag{D.4}$$

$$+\frac{\partial W}{\partial z}[\bar{A}][\sigma_3]\Big\}dVol - \int_{S(t)}[\bar{V}]^T W\Big\{[n][ST] + [\bar{A}][n][ST]\Big\}dS$$

$$= \int_{V(t)} W(\rho\dot{Q} + f_p[\dot{\varepsilon}]^T [\sigma_{ij}])\, dVol + \int_{S_q(t)} W(k_{xx}\frac{\partial T}{\partial x} n_x + k_{yy}\frac{\partial T}{\partial y} n_y + k_{zz}\frac{\partial T}{\partial z} n_z)dS$$

$$- \int_{S_p(t)} W(\text{internal energy})(\rho\bar{V}\cdot\hat{n})dS.$$

Note that the second and third terms in equation (D.4) are identically zero when the weighted momentum equations are satisfied. The integrands of the second and third integrals in equation (D.4) involve the linear momentum equation post-multiplied by $[\bar{V}]^T$, and the last integral represents the internal energy flux and includes all the terms involving $\dot{M}_p$. The surface S_q refers to the surfaces with specified heat-fluxes.

APPENDIX E

SPATIALLY DISCRETIZED LINEAR MOMENTUM EQUATION

In order to apply the C and A process to the linear momentum, we must discretize the region into a sub-set of NR regions or superelements. The unknown $[\bar{V}]$ within each of these regions is approximated by a piece-wise continuous function of the form,

$$[\bar{V}]_j = \begin{bmatrix} N_1 & 0 & 0 & N_2 & 0 & 0 & \cdots & N_{NP} & 0 & 0 \\ 0 & N_1 & 0 & 0 & N_2 & 0 & \cdots & 0 & N_{NP} & 0 \\ 0 & 0 & N_1 & 0 & 0 & N_2 & \cdots & 0 & 0 & N_{NP} \end{bmatrix} \begin{bmatrix} V_{1x} \\ V_{1y} \\ V_{1z} \\ \vdots \\ V_{NPx} \\ V_{NPy} \\ V_{NPz} \end{bmatrix} \qquad (E.1)$$

where NP(j) = number of nodal points in the jth region,

$\bar{V}_{ik}$ = the unknown value of the velocity at the ith node and in the kth direction,

N_i = an interpolation function in terms of the spatial variables.

Hence, all the integrals in equations (14) and (22) become a sum of integrals over each region. Note that the spatial variation of the velocity is now explicity given by the interpolation function.

Next, the weighting function is assumed to be approximated by a similar piece-wise continuous function, with a polynomial $N_i(x,y,z)$ associated with each node. Since equation (14) must be satisfied for each discrete weighting function N_i, one obtains a set of NP(j)*NDOF simultaneous equations for each region, where NDOF refers to the spatial degrees-of-freedom. Note that in a full F.E. approximation, the solution for <u>all</u> the unknown nodal values $(DOF*\sum_{j=1}^{NR} NP(j))$ must be solved <u>simultaneously</u>.

1. Elastic Behavior

The [L][U] displacement matrix in equation (14) can be written as,

$$[L][U] = \underset{NFG\times NDOF}{[L]} \quad \underset{NDOF\times MT}{[N]} \left[U_o + HV_i + \int_t^{t+\Delta t} \bar{V}_i(\tau)d(\tau) \right]_{MTx1} \qquad (E.2)$$

where HV_i = history of the velocity at the ith node up to time t,

$$= \int_{to}^{t} \bar{V}_i(\tau)d(\tau),$$

U_o = initial nodal displacements at time t_o,

MT = NDOF* * NP(j),

Δt = size of the current time-step,

NFG = digit which depends upon the geometry of the problem being solved.

Note that the only unknowns in equation (E.2) are the nodal velocities at the current time-step (the initial nodal velocities must be specified at time t_o).

The two remaining velocity terms are the [NLU] and $[\bar{A}]$ matrices which can be written as,

$$[NLU] = \begin{bmatrix} [IV]^T & [CX]^T & [CX] & [IV] \\ [IV]^T & [CY]^T & [CY] & [IV] \\ [IV]^T & [CZ]^T & [CZ] & [IV] \\ [IV]^T & [CX]^T & [CY] & [IV] \\ [IV]^T & [CX]^T & [CZ] & [IV] \\ [IV]^T & [CY]^T & [CZ] & [IV] \end{bmatrix}_{6x1} \tag{E.3}$$

$$\text{and} \quad [\bar{A}] = \begin{bmatrix} 0 & (UYIV) & (UZIV) \\ (VXIV) & 0 & (VZIV) \\ (WXIV) & (WYIV) & 0 \end{bmatrix} \tag{E.4}$$

$$\text{where } [IV] = \left[U_o + HV_i + \int_{t}^{t+\Delta t} \bar{V}_i(\tau)d\tau \right]_{MTx1}$$

$$[UX] = \left[\frac{\partial N_1}{\partial x} \; 0 \; 0 \; \frac{\partial N_2}{\partial x} \; 0 \; 0 \; \ldots \; \frac{\partial N_{NP}}{\partial x} \; 0 \; 0 \right]_{1xMT}$$

$$[VX] = \left[0 \; \frac{\partial N_1}{\partial x} \; 0 \; 0 \; \frac{\partial N_2}{\partial x} \; 0 \; \ldots \; 0 \; \frac{\partial N_{NP}}{\partial x} \; 0 \right]$$

* In equation (E.1), NDOF was set to a value of 3.

$$[WX] = [00\frac{\partial N_1}{\partial x} \quad 00\frac{\partial N_2}{\partial x} \quad \ldots \quad 00\frac{\partial N_{NP}}{\partial x}]$$

$$\ldots$$

$$[UZ] = [\frac{\partial N_1}{\partial z} \; 00 \; \frac{\partial N_2}{\partial z} \; 00 \; \ldots \; \frac{\partial N_{NP}}{\partial z} \; 0 \; 0]$$

$$[VZ] = [0 \; \frac{\partial N_1}{\partial z} \; 00 \; \frac{\partial N_2}{\partial z} \; 0 \; \ldots \; 0 \; \frac{\partial N}{\partial z}_{NP} \; 0]$$

$$[WZ] = [00 \; \frac{\partial N_1}{\partial z} \; 00 \; \frac{\partial N}{\partial z}_2 \; \ldots \; 00 \; \frac{\partial N}{\partial z}_{NP}]$$

$$[CX] = \begin{bmatrix} [UX] \\ [VX] \\ [WX] \end{bmatrix}_{3\times MT}$$

$$[CY] = \begin{bmatrix} [UY] \\ [VY] \\ [WY] \end{bmatrix}_{3\times MT}$$

$$[CZ] = \begin{bmatrix} [UZ] \\ [VZ] \\ [WZ] \end{bmatrix}_{3\times MT}$$

$$UYIV = [UY]\,[IV],$$

and

$WYIV = [WY]\,[IV]$. Note that NDOF was set equal to its maximum value of 3 in the above equations.

The remaining terms in equation (14) that must be spatially discretized are those involving the weighting function W. Using the previously defined interpolation functions, the terms involving the weighting function become the following,

$$\frac{\partial W}{\partial x}[D_x] = [CX]^T_{MT\times NDOF}\,[D_x]_{NDOF\times NFG}, \tag{E.5}$$

$$\frac{\partial W}{\partial y}[D_y] = [CY]^T\,[D_y], \tag{E.6}$$

$$\frac{\partial W}{\partial z}[D_z] = [CZ]^T\,[D_z], \tag{E.7}$$

$$W[F_B] = [N]^T\,[F_B]_{NDOF\times 1}, \tag{E.8}$$

$$W\,[\dot{\bar{V}}] = [N]^T\,[N]\,[\dot{\bar{V}}]_{MTx1} \tag{E.9}$$

$$W\,[n][ST] = [N]^T\,[n][ST] \tag{E.10}$$

and

$$W\,[\bar{V}] = [N]^T\,[N][\bar{V}]_{MTx1} \tag{E.11}$$

where $[N] = \begin{bmatrix} N_1 & 0 & 0 & N_2 & 0 & 0 & \cdots & N_{NP} & 0 & 0 \\ 0 & N_1 & 0 & 0 & N_2 & 0 & \cdots & 0 & N_{NP} & 0 \\ 0 & 0 & N_1 & 0 & 0 & N_2 & \cdots & 0 & 0 & N_{NP} \end{bmatrix}_{3xMT}$

Equations (E.1) through (E.11) are substituted into equation (14) to give the following set of spatially discretized equations,

$$\int_{V(j)} ([CX]^T\,[D_x] + [CY]^T\,[D_y] + [CZ]^T\,[D_z])[B]\,[IV]dVol$$

$$= -\int_{V(j)} \rho[N]^T[F_B]dVol - \int_{V(j)} \rho[N]^T\,[N][\bar{V}]dVol +$$

$$\int_{S(j)} [N]^T[n][ST]ds + \int_{V(j)} \rho([UX]^T+[VY]^T+[WZ]^T)_{1x3}\,dVol \tag{E.12}$$

$$+ \int_{S_p(j)} [N]^T[N][\bar{V}]\rho[n][N][\bar{V}]ds \quad -\sum_{k=1}^{11} [NL(k)],$$

where,

$$[B] = [L]_{NFGxNDOF}\,[N]_{NDOFxMT},$$

$$NL(1) = \int_{V(j)} [CX]^T\,[D_x]\,[NLU]_{NFGx1}\,dVol,$$

$$NL(2) = \int_{V(j)} [CY]^T\,[D_y]\,[NLU]\,dVol,$$

$$NL(3) = \int_{V(j)} [CZ]^T\,[D_z]\,[NLU]\,dVol,$$

$$NL(4) = \int_{V(j)} [CX]^T\,[\bar{A}]\,[D_x]\,[B]\,[IV]\,dVol,$$

$$NL(5) = \int_{V(j)} [CY]^T\,[\bar{A}]\,[D_y]\,[B]\,[IV]\,dVol,$$

$$NL(6) = \int_{V(j)} [CZ]^T [\bar{A}] [D_y] [B] [IV] \, dVol,$$

$$NL(7) = -\int_{V(j)} [\bar{A}] \, p \, ([UX]^T + [VY]^T + [WZ]^T)$$

$$NL(8) = -\int_{S(j)} [N]^T [\bar{A}] [n] [ST] \, ds,$$

$$NL(9) = \int_{V(j)} [CX]^T [\bar{A}] [D_x] [NLU] dVol,$$

$$NL(10) = \int_{V(j)} [CY]^T [\bar{A}] [D_y] [NLU] \, dVol,$$

$$NL(11) = \int_{V(j)} [CZ]^T [\bar{A}] [D_z] [NLU] \, dVol,$$

$V(j)$ = Volume of the jth region,

and

$S(j)$ = Surface area of the jth region with specified surface tractions.

Once the volume and surface integrations are performed, Equation (E.12) represents a set of non-linear, first-order, differential equations with respect to the MT unknown nodal velocities $[\bar{V}]$. Usually, the integrations are done using the numerical method of Gaussian Quadrature, with the number of integration points depending upon the interpolation function and the type of problem.

2. Fluid-Type Behavior

In addition to the discretized matrices given in the previous section, equation (22) involves several other velocity-dependent matrices. The most complex is the strain-rate of equation (21) which involves a matrix of products, with each product discretized to a series of matrix multiplications, i.e.,

$$\dot{NLU} = [(UVWX) \; (UVWY) \; (UVWZ) \; (UVWXY) \; (UVWXZ) \; (UVWYZ)]^T, \qquad (E.13)$$

where

$$UVWX = 2\{(UXIV) \; (UXV) + (VXIV) \; (VXV) + (WXIV) \; (WXV)\},$$

$$UVWY = 2\{(UYIV) \; (UYV) + (VYIV) \; (VYV) + (WYIV) \; (WYV)\},$$

$$UVWZ = 2\{(UZIV) \; (UZV) + (VZIV) \; (VZV) + (WZIV) \; (WZV)\},$$

$$UVWXY = (UXIV) \; (UYV) + (UXV) \; (UYIV) + (VXIV) \; (VYV) + (VXV) \; (VYIV) + (WXIV) \; (WYV) + (WXV) \; (WYIV),$$

$$UVWXZ = (UXIV)\ (UZV) + (UXV)\ (UZIV) + (VXIV)\ (VZV) + (VXV)\ (VZIV) + (WXIV)\ (WZV) + (WXV)\ (WZIV),$$

$$UVWYZ = (UYIV)\ (UZV) + (UYV)\ (UZIV) + (VYIV)\ (VZV) + (VYV)\ (VZIV) + (WYIV)\ (WZV) + (WYV)\ (WZIV),$$

$$UXV = [UX]\ [\bar{V}],$$

. . .

and

$$WZV = [WZ]\ [\bar{V}].$$

The remaining matrices are [H] and [$\dot{H}$] which involve the velocity implicitly through the $\sqrt{I_3}$ term. Using equations (19) and (E.4), and previous matrix definitions, the following determinant is obtained,

$$\sqrt{I_3} = \begin{vmatrix} (1 + UXIV) & (UYIV) & (UZIV) \\ (VXIV) & (1 + VYIV) & (VZIV) \\ (WXIV) & (WYIV) & (1 + WZIV) \end{vmatrix} . \qquad (E.14)$$

The time-derivative of this determinant can be written using equation (20) as,

$$\frac{\partial\sqrt{I_3}}{\partial t} = \begin{vmatrix} (UXV) & (UYV) & (UZV) \\ (VXV) & (VYV) & (VZV) \\ (WXV) & (WYV) & (WZV) \end{vmatrix} . \qquad (E.15)$$

Using the above discretized matrices, equation (22) can be written as the follow set of equations,

$$\int_{V(j)} ([CX]^T\ [ETAX] + [CY]^T\ [ETAY] + [CZ]^T\ [ETAZ])[B][\bar{V}]dVol$$

$$= -\int_{V(j)} \rho[N]^T\ [F_B]dVol - \int_{V(j)} \rho[N]^T\ [N]\ [\dot{\bar{V}}]dVol +$$

$$\int_{S(j)} [N]^T\ [n]\ [ST]ds + \int_{V(j)} (p+p_e)\ ([UX]^T+[VY]^T+[WZ]^T)\ dVol \qquad (E.16)$$

$$+ \int_{S_p(t)} [N]^T\ [N]\ [\bar{V}]\ \rho\ [\bar{n}]\ [N]\ [\bar{V}]dS$$

$$- \int_{V(j)} ([CX]^T\ [GX] + [CY]^T\ [GY] + [CZ]^T\ [GZ])\ ([B]\ [IV] - [H] - [e^E])dVol$$

$$+ \int_{V(j)} ([CX]^T\ [ETAX] + [CY]^T\ [ETAY] + [CZ]^T\ [ETAZ])\ ([\dot{e}^E] + [\dot{H}])dVol$$

$$-\sum_{k=1}^{23} [NLF(k)].$$

Note that in equation (E.16), the 6x1 matrices $[e^E]$, $[\dot{e}^E]$, $[\dot{H}]$ and $[H]$ involve array elements which are the matrix products of all the corresponding MT nodal values. The twenty-three NLF terms are not rewritten here since the forms are the same as before except with V→ V(j), S→ S(j), and equations (E.5) through (E.11) being substituted for the corresponding terms.

APPENDIX F

TEMPORALLY DISCRETIZED LINEAR MOMENTUM EQUATION

In both equation (E.12) and equation (E.16), the spatial variables have been integrated out, and the remaining unknowns are the MT nodal velocities as some continuous function of time. The next approximation is to replace the continuous time-behavior with a finite set of times for determining the nodal velocities.

1. Elastic Behavior

Equation (E.12) can be written in the standard form as

$$([KX]+[KY]+[KZ])[IV]= -[FB]+[FT] -[M][\dot{\bar{V}}]+[P]+[MF][\bar{V}]-\sum_{k=1}^{11}[NL(k)], \quad (F.1)$$

where,

$$[KX]= \int_{V(j)}[CX]^T[D_x][B]dVol,$$

$$[KY]= \int_{V(j)}[CY]^T[D_y][B]dVol,$$

$$[KZ]= \int_{V(j)}[CZ]^T[D_z][B]dVol,$$

$$[FB]=\int_{V(j)}\rho\ [N]^T[F_B]dVol,$$

$$[FT]= \int_{S(j)}[N]^T[N][ST]dS,$$

$$[M]=\int_{V(j)}\rho\ [N]^T[N]dVol,$$

$$[P]=\int_{V(j)}p\ ([UX]^T+[VY]^T+[WZ]^T)\ dVol,$$

and, $$[MF]=\int_{Sp(j)}[N]^T([N][\bar{V}][n])\ [N]dS.$$

We now assume a piecewise non-zero, time-dependent, weighting function WT(t), and approximate the time-dependent nodal velocities, using the following two equations, respectively.

$$WT(t)= \sum_{n=0}^{N_t} WT_n\ (t), \quad (F.2)$$

and $$[\bar{V}(t)]_{MTx1} =\Sigma NT_n(t)[\bar{V}(n)], \quad (F.3)$$

where N_t is the total number of time-steps selected for a particular problem, $[\bar{V}(n)]$ represents the MT nodal velocities at the time t_n, and $NT_n(t)$ is

the interpolation function for the nth time-element. Note that the $WT_n(t)$ functions are non-zero only over the nth time-element. Substituting equations (F.2) and (F.3) into equation (F.1) yields a set of N_t equations of the following form,

$$\int_{t_s}([KX]+[KY]+[KZ])\,[IV]WT_n(t)dt =$$

$$\int_{t_s}\left\{-[FB]+[FT]+[P]-\sum_{k=1}^{11}[NL(k)]\right\}WT_n(t)dt$$

$$-\left(\int_{t_s}[M]WT_n(t)[\dot{NT}_n(t)]dt\right)[\bar{V}(n)] \qquad (F.4)$$

$$+\left(\int_{t_s}[MF]WT_n(t)[NT_n(t)]dt\right)[\bar{V}(n)],$$

where t_s = time-span over which the nth weighting function is non-zero.

A wide variety of equations can be obtained from equation (F.4) depending upon the assumptions involving WT_n, NT_n and t_s. Also, the terms inside the spatial matrices may change with time due to either changing boundary conditions, or temperature-dependent material properties. Since the characteristic thermal time[29] can be several orders of magnitude less than the characteristic mechanical time[29] for impact problems, temperature-dependent material properties can be assumed constant during time steps small in comparison to the characteristic thermal time. The boundary conditions are usually matched by using sufficiently small time-steps associated with explicit solution schemes. However, for implicit schemes, which use larger time-steps, one may want to either use some interpolation scheme, or, to numerically integrate the time-integrals.

The author has developed explicit forms for equation (F.4) by assuming a quadratic interpolation function for all the spatial matrices. However, the resulting form involves a large number of matrices which must be numerically evaluated and stored. In retrospect, a faster method appears to be using program and input logic to flag certain boundary conditions which vary considerably over a time-step, and then use Gaussian Quadrature*

---

29. *B.A. Boley and J.H. Weiner, THEORY OF THERMAL STRESSES, Chap. 2, John Wiley and Sons, Inc., 1960*

* *A Gaussian order N will exactly integrate a polynomial of order 2N-1.*

to numerically integrate the corresponding time-integral. Hence, this latter approach will be used in the current study.

Because of the desire for large time-steps, the author selected an interpolation function for a quadratic time-element, i.e.,

$$[N_t(\bar{\tau})][\bar{V}(n)] = N_t(2n)[\bar{V}(2n)] + N_t(2n+1)[\bar{V}(2n+1)] + N_t(2n+2)[\bar{V}(2n+2)] \quad \text{(F.5)}$$

where $N_t(2n) = -\bar{\tau}(1-\bar{\tau})/2$,

$N_t(2n+1) = 1-\bar{\tau}^2$,

$N_t(2n+2) = \bar{\tau}(1+\bar{\tau})/2$,

$\bar{\tau} = 2(t-t_{middle})/\Delta t_n$,

Δt_n = time-step associated with the nth time-element,

$t_{middle} = t_n + \Delta t_n/2$

$[\bar{V}(2n)]$ = nodal velocities at start of time-step,

$[\bar{V}(2n+1)]$ = nodal velocities at middle of time-step,

and,

$[\bar{V}(2n+2)]$ = nodal velocities at the end of the time-step.

If we now assume that the nth weighting function is non-zero only over the nth time-element, then $t_s = \Delta t_n$ and the first term in equation (F.4) can be rewritten as,

$$\int_{t_s}([KX]+[KY]+[KZ])[IV]WT_n(t)dt =$$

$$\int_{t_{n-1}}^{t_n} WT_n(t)\ ([KX]+[KY]+[KZ])\Big\{[U_o]+\sum_{j=1}^{n-1}\frac{\Delta t_j}{2}\Big\{\int_{-1}^{1}\left(-\frac{\bar{\tau}(1-\bar{\tau})}{2}\right)d\bar{\tau}[N(2j)]$$

$$\int_{-1}^{1}(1-\tau^{-2})d\tau[N(2j+1)]+\int_{-1}^{1}\frac{\bar{\tau}(1+\bar{\tau})}{2}d\bar{\tau}[N(2j+2)]\Big\}+\int_{t_{n-1}}^{t}NT_n(\bar{t})[\bar{V}(n)]d\bar{t}\Big\}dt. \quad \text{(F.6)}$$

Substituting for the quadratic interpolation functions and N integrating, equation (F.6) becomes the following equation.

$$\int_{t_s}([KX] + [KY] + [KZ])\ [IV]\ WT_n(t)dt =$$

$$\frac{\Delta t}{2}_n \int_{-1}^{1} WT_n\ (\bar{\tau})\ ([KX] + [KY] + [KZ])d\bar{\tau}\ \{[U_o] \qquad (F.7)$$

$$+ \frac{\Delta t}{2}_n \sum_{j=1}^{n-1} \frac{\Delta t_j}{\Delta t_n} \left(\frac{1}{3}\ [\bar{V}(2j)] + \frac{4}{3}\ [\bar{V}(2j+1)] + \frac{1}{3}\ [\bar{V}(2j+2)]\right\}$$

$$+ \frac{\Delta t^2}{4}_n \left([\bar{K}(2n)]\,[\bar{V}(2n)] + [\bar{K}(2n+1)]\ \ [\bar{V}(2n+1)] + [\bar{K}(2n+2)]\ [\bar{V}(2n+2)]\right),$$

where, $[\bar{K}(2n)] = \int_{-1}^{1}([KX] + [KY] + [KZ])\left(\frac{5}{12} - \frac{\bar{\tau}}{4}^2 + \frac{\bar{\tau}}{6}^3\right)\ WT_n(\bar{\tau})d\bar{\tau},$

$$[\bar{K}(2n+1)] = \int_{-1}^{1} ([KX] + [KY] + [KZ])\ \left(\frac{2}{3} + \bar{\tau} - \frac{\bar{\tau}}{3}^3\right)\ WT_n(\bar{\tau})d\bar{\tau},$$

$$[\bar{K}(2n+2) = \int_{-1}^{1} ([KX] + [KY] + [KZ])\ \left(-\frac{1}{12} + \frac{\bar{\tau}}{4}^2 + \frac{\bar{\tau}}{6}^3\right)\ WT_n(\bar{\tau})d\bar{\tau}.$$

Utilizing equations (F.5) and (F.7), equation (F.4) can be rewritten as,

$$([\bar{K}(2n)] + [\bar{M}(2n)] - [\overline{MF}(2n)])\ [\bar{V}(2n)]$$

$$+([\bar{K}(2n+1)] + [\bar{M}(2n+1)] - [\overline{MF}(2n+1)])[\bar{V}(2n+1)]$$

$$+([\bar{K}(2n+2)] + [\bar{M}(2n+2)] - [\overline{MF}(2n+2)])\ [\bar{V}(2n+2)] \qquad (F.8)$$

$$= -[\overline{KV}] - [\overline{FB}] + [\overline{FT}] + [\bar{P}] - \sum_{k=1}^{11} [\overline{NL}(k)],$$

where, $[\bar{M}(2n)] = \frac{-2}{\Delta t_n^2} \int_{-1}^{1} [M]\ WT_n(\bar{\tau})(1-2\bar{\tau})\ d\bar{\tau},$

$$[\overline{M}(2n+1)] = \frac{-8}{\Delta t_n^2} \int_{-1}^{1} [M] WT_n(\bar{\tau}) \bar{\tau} d\bar{\tau},$$

$$[\overline{M}(2n+2)] = \frac{2}{\Delta t_n^2} \int_{-1}^{1} [M] WT_n(\bar{\tau}) (1+2\bar{\tau}) d\bar{\tau},$$

$$[\overline{MF}(2n)] = \frac{-1}{\Delta t_n} \int_{-1}^{1} [MF(\bar{\tau})] WT_n(\bar{\tau}) \{\bar{\tau}(1-\bar{\tau})\} d\bar{\tau},$$

$$[\overline{MF}(2n+1)] = \frac{2}{\Delta t_n} \int_{-1}^{1} [MF(\bar{\tau})] WT_n(\bar{\tau}) (1-\bar{\tau}^2) d\bar{\tau},$$

$$[\overline{MF}(2n+2)] = \frac{1}{\Delta t_n} \int_{-1}^{1} [MF(\bar{\tau})] WT_n(\bar{\tau}) \{\bar{\tau}(1+\bar{\tau})\} d\bar{\tau},$$

$$[\overline{KV}] = \int_{-1}^{1} WT_n(\bar{\tau}) ([KX]+[KY]+[KZ]) d\bar{\tau} *$$

$$\{\frac{2[U_o]}{\Delta t_n} + \sum_{j=1}^{n-1} \frac{\Delta t_j}{\Delta t_n} (\frac{1}{3}[\overline{V}(2j)]$$

$$+\frac{4}{3}[\overline{V}(2j+1)] + \frac{1}{3}[\overline{V}(2j+2)])\},$$

$$[\overline{FT}] = \frac{2}{\Delta t_n} \int_{-1}^{1} [FT] WT_n(\bar{\tau}) d\bar{\tau},$$

...

and,

$$[\overline{NL}(k)] = \frac{2}{\Delta t_n} \int_{-1}^{1} [NL(k)] WT_n(\bar{\tau}) d\bar{\tau}.$$

In the above equation, $[V(2n)]$ corresponds to the known nodal velocities at the start of the time-step, and hence there are twice MT number of unknowns and equations represented by equation (F.8). This is the disadvantage of the quadratic time-element, and for large MT considerably more computer time is required.

Equation (F.8) has been divided by the ratio $(\Delta t_n/2)^2$ to eliminate a similar factor which appeared as the coefficient of the $[\overline{K}]$ matrices. Also, the spatial matrices have been retained inside the time integrals so that, if necessary, time dependent behavior can be numerically integrated.

The last step is to select the weighting functions WT_n. In the Galerkin approximation, one selects the weight function to be the same function as used for the element-interpolation. This implies three functions which yield three matrix equations that can be combined into a single time-element. The single time-element is then combined with successive quadratic time-elements which yields the recursion relationships (see Chap. 17 of reference 8). The disadvantage of this approach is that a series of simultaneous equations must be solved at each time-step. To the author's knowledge commercial FE programs use recursion relationships which assume only a single weighting function that is non-zero over a single-time element. Furthermore, most programs use linear time-elements which yield the familiar forward difference, central difference and backward difference type of equations.

If the weighting function weights over more than one time-step, and a linear time-element is assumed, then higher level schemes, such as Houbolt's Method,* are obtained. The advantage of the higher level scheme over the quadratic time-element is that there are only MT unknowns per time-step. However, it appears that the number of stored matrices for the three-level scheme is about the same as that for the quadratic time-element. Therefore, computational speed involves a trade-off between more storage and CPU time per time-step for the quadratic time-element versus fewer time-steps required to solve a problem.

One should note that the usual displacement formulation of the linear momentum equation involves a second-order equation in time, and a quadratic time-element is used in many current FE programs. The corresponding recursion relationship is a three-level scheme[7] with a variety of forms similar to Newmark's general algorithm.[30] Some FE programs use a four-level scheme, where there is still only MT unknowns, and special "starting" algorithms must be used to determine the unknowns at the first three time-nodes.

In order to perform numerical experiments, the author assumed that the spatial matrices of the left-hand-side of equation(F.8) are independent of time within a time-step, and equation (F.8) was rewritten in the following form,

$$[A][\bar{V}(2n+2)]+[B][\bar{V}(2n+1)]+[C][\bar{V}(2n)]=[CF],\ n=0,1,\ldots NT \qquad (F.9)$$

See Swanson Analysis Systems, Inc. Theoretical Manual for application of this method to a varity of FE programs, 2nd Ed, 1983

[30] *N.M. Newmark, "A Method for Computation of Structural Dynamics", Proc. Am. Soc. Civil Eng., 85, EMS, pp. 67-94, 1959.*

where the [A],[B],[C] and [CF] matrices take different forms depending upon the weighting function assumption.

When a single weighting function is assumed over the time-step, equation (F.9) becomes the usual three-level scheme with the following change of the indices: 2n+2→n+1, 2n+1→n, and 2n→n-1, with n=1, 2,...,NT. Table F-1 lists six weighting functions selected*by the author and the corresponding matrix elements. Note that the $[\overline{MF}]$ terms have been neglected, $[K]=[KX]+[KY]+[KZ]$, and the [F] matrix represents the right-hand-side of equation (F.8). All matrices are evaluated at the middle of the time-step Δt.

When three weighting functions are assumed over the time-step the following form of the weighted residuals is obtained for a single quadratic time-element,

$$\begin{bmatrix} K_{11} & K_{12} & K_{13} \\ K_{21} & K_{22} & K_{23} \\ K_{31} & K_{32} & K_{33} \end{bmatrix} \begin{bmatrix} \overline{V}(2n) \\ \overline{V}(2n+1) \\ \overline{V}(2n+2) \end{bmatrix} = \begin{bmatrix} K_{1n}F(2n) \\ K_{2n}F(2n+1) \\ K_{3n}F(2n+2) \end{bmatrix} \qquad (F.10)$$

where the K_{ij} values are dependent upon the assumed weighting functions. In this set of equations, the $\overline{V}(2n)$ are known (either the initial values, or, from the previous time-step). Therefore, equation (F.10) can be re-written as

$$\begin{bmatrix} K_{22} & K_{23} \\ K_{32} & K_{33} \end{bmatrix} \begin{bmatrix} \overline{V}(2n+1) \\ \overline{V}(2n+2) \end{bmatrix} = \begin{bmatrix} K_{2n}\ F(2n+1)-K_{21}\overline{V}(2n) \\ K_{3n}\ F(2n+2)-K_{31}\overline{V}(2n) \end{bmatrix} \qquad (F.11)$$

2MTx1

As discussed earlier, this larger system of equations is justified only if either a better approximation is obtained for the same CPU time, or the same approximation is obtained with less CPU time than the single weighting function approach.

In order to evaluate the above K_{ij} coefficients, the author assumed the following two sets:A. A true Galerkin approximation using the second through the fourth weighting functions given in Table F-1, and B. three linear functions associated with the last two weighting functions given in Table F-1. The resulting K_{ij} coefficients are given in Table F-2. Again, the $[\overline{MF}]$ terms have been neglected.

These are the same as those used in reference 28 so that a comparison can be made with the standard displacement approach.

Table F-1 Possible Weighting Functions and the Corresponding MTxMT Matrices

Function	[A]	[B]	[C]	[CF]
1. Constant =1	$[M]/\Delta t^2$	$[K]/3$	$[K]/6 - [M]/\Delta t^2$	$[F]/\Delta t^*$
2. $-\bar{\tau}(1-\bar{\tau})/2$	$-[K]/60-[M]/\Delta t^2$	$13[K]/30+4[M]/\Delta t^2$	$[K]/12-3[M]/\Delta t^2$	$[F]/\Delta t$
3. $(1-\bar{\tau}^2)$	$-[K]/60+[M]/\Delta t^2$	$[K]/3$	$11[K]/60-[M]/\Delta t^2$	$[F]/\Delta t$
4. $\bar{\tau}(1+\bar{\tau})/2$	$[K]/12+3[M]/\Delta t^2$	$11[K]/15-4[M]/\Delta t^2$	$11[K]/60+[M]/\Delta t^2$	$[F]/\Delta t$
5. $-\bar{\tau}, t_{n-1} \le t \le t_n$ $\bar{\tau}, t_n \le t \le t_{n+1}$	$[K]/48+[M]/\Delta t^2$	$[K]/3$	$7[K]/48-[M]/\Delta t^2$	$[F]/\Delta t$
6. $1+\bar{\tau}, t_{n-1} \le t \le t_n$ $1-\bar{\tau}, t_n \le t \le t_{n+1}$	$-[K]/96+[M]/\Delta t^2$	$[K]/3$	$3[K]/16-[M]/\Delta t^2$	$[F]/\Delta t$

*$\Delta t = t_{n+1} - t_{n-1}$

Table F-2 Coefficients for Equation (F.11) Associated with Two Sets of Weighting Functions

Coefficient	Set A	Set B
K_{21}	$\frac{11[K(2n)]}{90} - \frac{2[M(2n)]}{3\Delta t^2}$	$\frac{3[K(2n)]}{32} + \frac{[M(2n)]}{2\Delta t^2}$
K_{22}	$\frac{2[K(2n+1)]}{9}$	$\frac{[K(2n+1)]}{6}$
K_{23}	$-\frac{[K(2n+2)]}{90} + \frac{2[M(2n+2)]}{3\Delta t^2}$	$-\frac{[K(2n+2)]}{192} + \frac{[M(2n+2)]}{2\Delta t^2}$
K_{31}	$\frac{11[K(2n)]}{180} + \frac{[M(2n)]}{3\Delta t^2}$	$\frac{43[K(2n)]}{480} + \frac{[M(2n)]}{6\Delta t^2}$
K_{32}	$\frac{11[K(2n+1)]}{45} - \frac{4[M(2n+1)]}{3\Delta t^2}$	$\frac{3[K(2n+1)]}{10} - \frac{4[M(2n+1)]}{3\Delta t^2}$
K_{33}	$\frac{[K(2n+2)]}{36} + \frac{[M(2n+2)]}{\Delta t^2}$	$\frac{13[K(2n+2)]}{480} + \frac{7[M(2n+2)]}{6\Delta t^2}$
K_{2n}	$2/3\Delta t$	$1/2\Delta t$
K_{3n}	$1/3\Delta t$	$1/2\Delta t$

2. Fluid-Type Behavior

As discussed in Appendix E, the most complicated matrix involves the strain-rate matrix of equation (E.13). Inspection of this equation shows that each array-element involves the velocity matrix [V]. Furthermore, since each matrix product within the (UVW...) type of array-element corresponds to a scalar, the (UXV) (UZIV) type of items can be rewritten as (UZIV) (UXV), etc. Therefore, each array-element can be considered as post multiplied by [V] and equation (E.13) can be rewritten as

$$[\underset{6xMT}{NL\dot{U}}] = [\underset{6xMT}{UXYZ}]\,[V]. \qquad (F.12)$$

where $[\underset{1xMT}{UXYZ(1)}] = 2\,\{(UXIV)\,[UX] + (VXIV)\,[VX] + (WXIV)\,[WX]\},$

$$[UXYZ(2)] = 2\,\{(UYIV)\,[UY] + (VYIV)\,[VY] + (WYIV)\,[WY]\},$$

$$[UXYZ(3)] = 2\,\{(UZIV)\,[UZ] + (VZIV)\,[VZ] + (WZIV)\,[WZ]\},$$

$$[UXYZ(4)]=(UXIV)[UY]+(UYIV)[UX]+(VXIV)[VY]+(VYIV)[VX]+(WXIV)[WY]+(WYIV)[WX],$$

$$[UXYZ(5)]=(UXIV)[UZ]+(UZIV)[UX]+(VXIV)[VZ]+(VZIV)[VX]+(WXIV)[WZ]+(WZIV)[WX],$$

$$[UXYZ(6)]=(UYIV)[UZ]+(UZIV)[UY]+(VYIV)[VZ]+(VZIV)[VY]+(WYIV)[WZ]+(WZIV)[WY].$$

Multiplying equation (E.16) by the nth weighting function, substituting equations (F.3), (F.5) and (F.12), integrating over time and rearranging terms yields the following equation,

$$\begin{aligned}&([\overline{KE}(2n+2)]+[\overline{G}(2n+2)]+[\overline{M}(2n+2)]-[\overline{MF}(2n+2)]+[\overline{KEN}(2n+2)])\\&[\overline{V}(2n+2)]+([\overline{KE}(2n+1)]+[\overline{G}(2n+1)]+[\overline{M}(2n+1)]-[\overline{MF}(2n+1)]\\&+[\overline{KEN}(2n+1)])[\overline{V}(2n+1)]+([\overline{KE}(2n)]+[\overline{G}(2n)]+[\overline{M}(2n)]\\&-[\overline{MF}(2n)]+[\overline{KEN}(2n)])[\overline{V}(2n)]=-[\overline{GV}]-[\overline{FB}]+[\overline{FT}]\\&+[\overline{PE}]+[\overline{GXYZ}]+[\overline{ETAXYZ}]-\sum_{k=1}^{20}[\overline{NLF}(k)]\\&\qquad k \neq 4,5,6\end{aligned} \qquad (F.13)$$

where $[\overline{KE}(2n)] = \frac{1}{\Delta t_n}\int_{-1}^{1}([KEX] + [KEY] + [KEZ])\, WT_n(\bar{\tau})\{-\bar{\tau}(1-\bar{\tau})\}d\bar{\tau}$,

$$[\overline{KE}(2n+1)] = \frac{2}{\Delta t_n}\int_{-1}^{1}([KEX] + [KEY] + [KEZ])\, WT_n(\bar{\tau})(1-\bar{\tau}^2)d\bar{\tau},$$

$$[\overline{KE}(2n+2)] = \frac{1}{\Delta t_n}\int_{-1}^{1}([KEX] + [KEY] + [KEZ])\, WT_n(\bar{\tau})\bar{\tau}(1+\bar{\tau})d\bar{\tau},$$

$$[\overline{KEN}(2n)] = \frac{1}{\Delta t_n}\int_{-1}^{1}([KENX] + [KENY] + [KENZ])\, WT_n(\bar{\tau})\{-\bar{\tau}(1-\bar{\tau})\}d\bar{\tau},$$

$$[\overline{KEN}(2n+1)] = \frac{2}{\Delta t_n}\int_{-1}^{1}([KENX] + [KENY] + [KENZ])\, WT_n(\bar{\tau})(1-\bar{\tau}^2)d\bar{\tau},$$

$$[\overline{KEN}(2n+2)] = \frac{1}{\Delta t_n}\int_{-1}^{1}([KENX] + [KENY] + [KENZ])\, WT_n(\bar{\tau})\bar{\tau}(1+\bar{\tau})d\bar{\tau},$$

$$[\overline{G}(2n)] = \int_{-1}^{1}[GXYZ]\left(\frac{5}{12}-\frac{\bar{\tau}^2}{4}+\frac{\bar{\tau}^3}{6}\right)WT_n(\bar{\tau})d\bar{\tau},$$

$$[\overline{G}(2n+1)] = \int_{-1}^{1}[GXYZ]\left(\frac{2}{3}+\bar{\tau}-\frac{\bar{\tau}^3}{3}\right)WT_n(\bar{\tau})d\bar{\tau},$$

$$[\overline{G}(2n+2)] = \int_{-1}^{1}[GXYZ]\left(\frac{-1}{12}+\frac{\bar{\tau}^2}{4}+\frac{\bar{\tau}^3}{6}\right)WT_n(\bar{\tau})d\bar{\tau},$$

$$[\overline{GV}] = \int_{-1}^{1}WT_n(\bar{\tau})[GXYZ]d\bar{\tau} * \left\{2[U_o] + \sum_{j=1}^{n-1}\frac{\Delta t_j}{\Delta t_n}\left(\frac{1}{3}[\overline{V}(2j)] + \frac{4}{3}[\overline{V}(2j+1)] + \frac{1}{3}[\overline{V}(2j+2)]\right)\right\}$$

and

$$[\overline{PE}] = \frac{2}{\Delta t_n} \int_{-1}^{1} \{[PEX]+[PEY]+[PEZ]\} WT_n(\bar{\tau})\, d\bar{\tau},$$

$$[\overline{GXYZ}] = \frac{2}{\Delta t_n} \int_{-1}^{1} \{[CX]^T[GX] + [CY]^T[GY] + [CZ]^T[GZ]\}[\varepsilon^E] dVol\ WT_n(\bar{\tau})\, d\bar{\tau},$$

$$[\overline{ETAXYZ}] = \frac{2}{\Delta t_n} \int_{-1}^{1} [ETAXYZ] WT_n(\bar{\tau})\, d\bar{\tau},$$

$$[\overline{NLF(k)}] = \frac{2}{\Delta t_n} \int_{-1}^{1} [NLF(k)] WT_n(\bar{\tau})\, d\bar{\tau},$$

$$[KEX] = \int_{V(j)} [CX]^T[ETAX][B] dVol,$$

$$[KEY] = \int_{V(j)} [CY]^T[ETAY][B] dVol,$$

$$[KEZ] = \int_{V(j)} [CZ]^T[ETAZ][B] dVol,$$

$$[KENX] = \int_{V(j)} [CX]^T \{([I]+[\bar{A}])[ETAX][UXYZ] + [\bar{A}][ETAX][B]\} dVol,$$

$$[KENY] = \int_{V(j)} [CY]^T \{([I]+[\bar{A}])[ETAY][UXYZ] + [\bar{A}][ETAY][B]\} dVol,$$

$$[KENZ] = \int_{V(j)} [CZ]^T \{([I]+[\bar{A}])[ETAZ][UXYZ] + [\bar{A}]\ [ETAZ][B]\} dVol,$$

$$[PEX] = \int_{V(j)} (p+p_e)[UX]^T\, dVol,$$

$$[PEY] = \int_{V(j)} (p+p_e)[UY]^T\, dVol,$$

$$[PEZ] = \int_{V(j)} (p+p_e)[UZ]^T\, dVol,$$

$$[GXYZ] = \int_{V(j)} ([CX]^T[GX] + [CY]^T[GY] + [CZ]^T[GZ])[B] dVol,$$

$$[ETAXYZ]=\int_{V(j)}([CX]^T[ETAX]+[CY]^T[ETAY]+[CZ]^T[ETAZ])[\dot{\varepsilon}^E]dVol.$$

Note that the nonlinear terms NLF(k), k=4,5,6,21, 22 and 23, in equation (E.16) have been rearranged into the $[\overline{KEN}]$ terms of the above equation. Also, equation (F.13) has exactly the same form as equation (F.8), except that the velocity coefficient-matrices $[\overline{KE}]$ and $[\overline{KEN}]$ depend upon the unknown velocity. Hence, even if all the [NLF]matrices are neglected, equation (F.13) can only be solved via an iterative process.

For the special case of no strain-hardening i.e., [GXYZ]≡0, the $[\overline{G}]$ and $[\overline{GV}]$ matrices are identically zero and equation (F.13) contains a common Δt_n term which can be canceled out. The resulting equation corresponds to the familar first-order type of recursive equation.

Since the form of equation (F.13) is similar to equation (F.8), the explicit equations for the same assumptions and specific weighting function, or set of weighting functions, will be the same. Therefore, the coefficient matrices given in Tables F-1 and F-2 also apply to equation (F.13) if the [K] matrix is replaced by the $[\overline{GXYZ}]$ matrix, and the $[\overline{KE}]$, $[\overline{KEN}]$, and $[\overline{MF}]$ matrices are neglected.

For the more general problems, the [K] matrix of Tables F-1 and F-2 must be replaced by three matrices corresponding to [G],[KE] and $[\overline{KEN}]$. Using the same functions as previously for the elastic type of behavior, Table F-3 and F-4 list the corresponding [A],[B] and [C] matrices for usage in equation (F.9). Similarly, Tables F-5 and F-6 list the K_{ij} coefficients for usage in equation (F.11) when applied to fluid-type behavior.

Table F-3 Possible Weighting Functions and the Corresponding MTxMT Matrices for Fluid-Type Behavior and Equation (F.9)

Function: Constant = 1

$$[A] = \frac{1}{6\Delta t}([KE]+[KEN]) + \frac{[M]}{\Delta t^2}$$

$$[B] = \frac{2}{3\Delta t}([KE]+[KEN]) + \frac{[GXYZ]}{3}$$

$$[C] = \frac{1}{6\Delta t}([KE]+[KEN]) + \frac{[GXYZ]}{6} - \frac{[M]}{\Delta t^2}$$

Function: $-\bar{\tau}(1-\bar{\tau})/2$

$$[A] = \frac{-1}{5\Delta t}([KE]+[KEN]) - \frac{[GXYZ]}{60} - \frac{[M]}{\Delta t^2}$$

$$[B] = \frac{2}{5\Delta t}([KE]+[KEN]) + \frac{13}{30}[GXYZ] + \frac{4}{\Delta t^2}[M]$$

$$[C] = \frac{4}{5\Delta t}([KE]+[KEN]) + \frac{[GXYZ]}{12} - \frac{3}{\Delta t^2}[M]$$

Function: $(1-\bar{\tau}^2)$

$$[A] = \frac{1}{10\Delta t}([KE]+[KEN]) - \frac{[GXYZ]}{60} + \frac{[M]}{\Delta t^2}$$

$$[B] = \frac{4}{5\Delta t}([KE]+[KEN]) + \frac{[GXYZ]}{3}$$

$$[C] = \frac{1}{10\Delta t}([KE]+[KEN]) + \frac{11}{60}[GXYZ] - \frac{[M]}{\Delta t^2}$$

Table F-4 Possible Weighting Functions and the corresponding MTxMT Matrices for Fluid-Type Behavior and Equation (F.9)

Function: $\bar{\tau}\ (1+\bar{\tau})/2$

$$[A]= \frac{4}{5\Delta t}([KE]+[KEN])+\frac{[GXYZ]}{12}+\frac{3[M]}{\Delta t^2}$$

$$[B]= \frac{2}{5\Delta t}([KE]+[KEN])+\frac{11}{15}[GXYZ]-\frac{4}{\Delta t^2}[M]$$

$$[C]= \frac{-1}{5\Delta t}([KE]+[KEN])+\frac{11}{60}[GXYZ]+\frac{[M]}{\Delta t^2}$$

Function: $-\bar{\tau},\ t_{n-1}\leq t\leq t_n;\bar{\tau},\ t_n\leq t\leq t_{n+1}$

$$[A]= \frac{1}{4\Delta t}([KE]+[KEN])+\frac{[GXYZ]}{48}+\frac{[M]}{\Delta t^2}$$

$$[B]= \frac{1}{2\Delta t}([KE]+[KEN])+\frac{[GXYZ]}{3}$$

$$[C]= \frac{1}{4\Delta t}([KE]+[KEN])+\frac{}{48}[GXYZ]-\frac{[M]}{\Delta t^2}$$

Function: $1+\bar{\tau},\ t_{n-1}\leq t\leq t_n;\ 1-\bar{\tau},\ t_n\leq t\leq t_{n+1}$

$$[A]= \frac{1}{12\Delta t}([KE]+[KEN])-\frac{[GXYZ]}{96}+\frac{[M]}{\Delta t^2}$$

$$[B]= \frac{5}{6\Delta t}([KE]+[KEN])+\frac{[GXYZ]}{3}$$

$$[C]= \frac{1}{12\Delta t}([KE]+[KEN])+\frac{3}{16}[GXYZ]-\frac{[M]}{\Delta t^2}$$

Table F-5 Coefficients for Equation (F.11) Associated with Set A of the Weighting Functions

Coefficient	
K_{21}	$\frac{11}{90}[G(2n)]+\frac{1}{15\Delta t_n}([KE(2n)]+[KEN(2n)])-\frac{2[M(2n)]}{3\Delta t_n^2}$
K_{22}	$\frac{2}{9}[G(2n+1)]+\frac{8}{15\Delta t_n}([KE(2n+1)]+[KEN(2n+1)])$
K_{23}	$-\frac{[G(2n+2)]}{90}+\frac{1}{15\Delta t_n}([KE(2n+2)]+[KEN(2n+2)])+\frac{2[M(2n+2)]}{3\Delta t_n^2}$
K_{31}	$\frac{11}{180}[G(2n)]-\frac{1}{15\Delta t_n}([KE(2n)]+[KEN(2n)]+\frac{[M(2n)]}{3\Delta t_n^2}$
K_{32}	$\frac{11}{45}[G(2n+1)]+\frac{2}{15\Delta t_n}([KE(2n+1)]+[KEN(2n+1)])-\frac{4[M(2n+1)]}{3\Delta t_n^2}$
K_{33}	$\frac{[G(2n+2)]}{36}+\frac{4}{15\Delta t_n}([KE(2n+2)]+[KEN(2n+2)])+\frac{[M(2n+2)]}{\Delta t_n^2}$
K_{2n}	$2/(3\Delta t_n)$
K_{3n}	$1/(3\Delta t_n)$

$G(2n)$, $G(2n+1)$, $G(2n+2) \equiv [GXYZ]$ evaluated at times t_{2n}, t_{2n+1}, and t_{2n+2} respectively.

Table F-6 Coefficients for Equation (F.11) Associated with Set B of the Weighting Functions

Coefficient

K_{21} $\frac{3}{32}[G(2n)]+\frac{1}{24\Delta t_n}([KE(2n)]+[KEN(2n)])+\frac{[M(2n)]}{2\Delta t_n^2}$

K_{22} $\frac{[G(2n+1)]}{6}+\frac{5}{12\ t_n}([KE(2n+1)]+[KEN(2n+1)])$

K_{23} $-\frac{[G(2n+2)]}{192}+\frac{1}{24\Delta t_n}([KE(2n+2)]+[KEN(2n+2)])+\frac{[M(2n+2)]}{2\Delta t_n^2}$

K_{31} $\frac{43}{480}G(2n)-\frac{1}{24\Delta t_n}([KE(2n)]+[KEN(2n)])+\frac{[M(2n)]}{6\Delta t_n^2}$

K_{32} $\frac{3}{10}[G(2n+1)]+\frac{1}{4\Delta t_n}([KE(2n+1)]+[KEN(2n+1)])-\frac{4}{3\Delta t_n^2}[M(2n+1)]$

K_{33} $\frac{13}{480}[G(2n+2)]+\frac{7}{24\Delta t_n}([KE(2n+2)]+[KEN(2n+2)])+\frac{7\ [M(2n+2)]}{6\Delta t_n^2}$

K_{2n} $1/(2\Delta t_n)$

K_{3n} $1/(2\Delta t_n)$

APPENDIX G

SPATIALLY AND TEMPORALLY DISCRETIZED ENERGY EQUATION

The discretized linear momentum equation contains coefficients and a pressure term which depend upon the temperature. The temperature explicitly appears in the energy equation (D.4), and therefore, the momentum and energy equations are coupled together. The fully discretized velocity can be utilized directly in equation (D.4), and the temperature is spatially discretized using the following approximation,

$$T(x,y,z,t) \cong \sum_{j=1}^{NR} \sum_{i=1}^{NPT(j)} NTE_i(x,y,z)\, T_i(t) \qquad (G.1)$$

$$\cong \sum_{j=1}^{NR} [NTE]\,[T(t)]$$

where NTE = a trial function in terms of the spatial variables,
$T_i(t)$ = the unknown value of the temperature at the ith node,
NPT(j) = number of temperature-nodal points in the jth region.

Equation (23) is spatially discretized by substituting equation (G.1) to yield

$$\frac{\partial}{\partial t}(\text{thermal part of EOS}) = \{\frac{dB}{dT} + \frac{\partial B_1}{\partial T}\,[NTE][T]$$

$$+ B_1 + \frac{\partial B_2}{\partial T}\,[T]^T\,[NTE]^T\,[NTE]\,[T] \qquad (G.2)$$

$$+ 2B_2\,[NTE][T]\}[NTE][\dot{T}] + (\frac{\partial B_1}{\partial \sqrt{I_3}}\frac{\partial \sqrt{I_3}}{\partial t} + \frac{\partial B_2}{\partial \sqrt{I_3}}\frac{\partial \sqrt{I_3}}{\partial t}\,[T]^T[NTE]^T)[NTE][T].$$

The spatial gradients of the temperature are discretized into the following forms

$$K_{xx}\frac{\partial T}{\partial x}\,n_x + K_{yy}\frac{\partial T}{\partial y}\,n_y + K_{zz}\frac{\partial T}{\partial z}\,n_z = (K_{xx}\,n_x[TX]$$

$$+ K_{yy}\,n_y[TY] + K_{zz}\,n_z[TZ])\,[T], \qquad (G.3)$$

$$\nabla W\cdot(k_{xx}\frac{\partial T}{\partial x} + k_{yy}\frac{\partial T}{\partial y} + K_{zz}\frac{\partial T}{\partial z}) = [BT]^T\,[KT]\,[BT]\,[T], \qquad (G.4)$$

where $[TX] = [\frac{\partial}{\partial x}\,NTE_1 \cdots \frac{\partial}{\partial x}\,NTE_{TNP}]$,

$[TY] = [\frac{\partial}{\partial y}\,NTE_1 \cdots \frac{\partial}{\partial y}\,NTE_{TNP}]$,

$[TZ] = [\frac{\partial}{\partial z}\,NTE_1 \cdots \frac{\partial}{\partial z}\,NTE_{TNP}]$,

$$[BT] = \left[[TX]\ [TY]\ [TZ]\right]^{T}_{TNPx3},$$

$$[KT] = \begin{bmatrix} K_{xx} & 0 & 0 \\ 0 & K_{yy} & 0 \\ 0 & 0 & K_{zz} \end{bmatrix}.$$

The last term that must be discretized is the product involving the strain-rate and stress. Using previously defined matrices, the strain-rate matrix becomes,

$$[\dot{\varepsilon}]^{T} = [\bar{V}]^{T}\,[B]^{T} + [\bar{V}]^{T}\,[UXYZ]^{T}. \qquad (G.5)$$

The stress matrix depends upon the condition of the material. For elastic behavior, the stress matrix can be written as,

$$[\sigma_{ij}]_{NFGx1} = [C_{ij}]_{NFGxNFG}\,[\varepsilon] - [p], \qquad (G.6)$$

where C_{ij} = elastic compliances,*

$$[\sigma_{ij}] = [\sigma_{xx}\ \sigma_{yy}\ \sigma_{zz}\ \sigma_{xy}\ \sigma_{xz}\ \sigma_{yz}]^{T},$$

$$[p] = [p\ p\ p\ 0\ 0\ 0]^{T},$$

when NFG equals six.

Therefore, the matrix product for elastic behavior is

$$[\dot{\varepsilon}]^{T}\,[\sigma_{ij}] = [\bar{V}]^{T}\,([B]^{T} + [UXYZ]^{T} \qquad (G.7)$$
$$\{[C_{ij}]\,([B]\,[IV] + [NLU]) - [p]\}.$$

For fluid-type of behavior, equations (15) through (17) are used to yield the following stress matrix for <u>loading</u> behavior,

$$[\sigma_{ij}] = [G]\,([\varepsilon] - [\varepsilon^{E}]) + [ETA]\,([\dot{\varepsilon}] - [\dot{\varepsilon}^{E}]) - [p_{T}], \qquad (G.8)$$

where $[G] = G_{T}\begin{bmatrix} 2[I] & [0] \\ [0] & [I] \end{bmatrix}_{6x6}$

*The previously defined matrices $[D_i]$, i=x,y,z, are for the special case of an isotropic material.

$$[ETA] = n_{eff} \begin{bmatrix} 2[I] & [0] \\ [0] & [I] \end{bmatrix}_{6x6}$$

$$[p_T] = [p_T p_T p_T 000]^T, \qquad p_T = p + p_e,$$

when NFG equals six. The corresponding matrix product becomes,

$$[\dot{\varepsilon}]^T [\sigma_{ij}] = [\bar{V}]^T([B]^T + [UXYZ]^T)\Big\{[G]([B]\ [IV] + [NLU] - [\varepsilon^E])$$
$$+ [ETA]\{([B] + [UXYZ])\ [\bar{V}] - [\dot{\varepsilon}^E]\} - [p_T]\Big\}. \qquad (G.9)$$

If we now assume that the weighted momentum equations are zero for the discretized values of temperature and velocity, and the weighting function equals the trial function, energy equation (D.4) can be written in the following form for each region,

$$\Big\{\int_{V(j)} \rho\ (a_1(T) + a_2(T)\ [NTE]\ [T] + \frac{\partial B_2}{\partial T^2}\ [T]^T\ [NTE]^T\ [NTE]\ [T])$$
$$[NTE]^T\ [NTE] dVol\Big\}[\dot{T}] + \Big\{\int_{V(j)} \rho(a_3(T) + a_4(T)\ [T]^T$$
$$[NTE])\ [NTE]^T\ [NTE] dVol + \int_{V(j)} [BT]\ [KT]\ [BT] dVol + \int_{S_b(j)} \bar{h}\ [NTE]^T\ [NTE] dS$$
$$+ \int_{S_c(j)} a(T,T_\infty)\ [NTE]^T\ [NTE] dS\Big\}\ [T] = \int_{S_a(j)} [NTE]^T\ q dS \qquad (G.10)$$
$$+ \int_{V(j)} \rho [NTE]^T\ \dot{Q} dVol + \int_{S_b(j)} \bar{h}\ T_\infty\ [NTE]^T dS$$
$$- \int_{S_p(t)} [NTE]^T\ (\text{Internal energy})\ (\rho[N]^T\ [\bar{V}]\cdot\hat{n}) dS$$
$$+ \int_{S_c(j)} [NTE]^T\ a(T,T_\infty)\ T_\infty dS + \sum_{k=1}^{5}\ [FV(k)],$$

where $a(T,T_\infty) = \alpha_e F_f \sigma_{SB} \left([T]^T [NTE]^T [NTE] [T] + T_\infty^2\right) * ([NTE] [T] + T_\infty)$,

$$a_1(T) = \frac{dB}{dT} + B_1,$$

$$a_2(T) = 2B_2 + \frac{\partial B_1}{\partial T},$$

$$a_3(T) = \frac{\partial B_1}{\partial \sqrt{I_3}} \frac{\partial \sqrt{I_3}}{\partial t},$$

$$a_4(T) = \frac{\partial B_2}{\partial \sqrt{I_3}} \frac{\partial \sqrt{I_3}}{\partial t},$$

α_e = effective emissivity,

F_f = form factor,

σ_{SB} = Stephen-Boltzmann constant,

T_∞ = far-field environmental temperature,

$\bar{h}$ = effective film-coefficient,

$S_q = S_a + S_b + S_c$,

$S_a(j)$ = boundary of jth region which has a conductive flux q,

$S_b(j)$ = boundary of jth region which has a convective flux,

$S_c(j)$ = boundary of jth region which has a radiation-flux,

$$[FV(1)] = -\int_{V(j)} \rho [NTE]^T [\bar{V}]^T [N]^T [F_B] dVol,$$

$$[FV(2)] = -\int_{V(j)} \rho [NTE]^T [\bar{V}]^T [N]^T [\dot{\bar{V}}] dVol,$$

$$[FV(3)] = \int_{S(j)} [NTE]^T [\bar{V}]^T [N]^T [n] [ST] dS,$$

$$[FV(4)] = \int_{S(j)} [NTE]^T [\bar{V}]^T [N]^T [\bar{A}] [n] [ST] dS,$$

$$[FV(5)] = \int_{V(j)} \rho [NTE]^T (f_p - f_e) [\dot{\varepsilon}]^T [\sigma_{ij}] dVol.$$

The flux q is either specified on an exterior boundary of the body, or evaluated from an adjacent region using equation (G.3). The product $[\dot{\varepsilon}]^T [\sigma_{ij}]$ is given by either equation (G.7) or (G.9) depending upon the material condition. The velocity variable is implicitly contained within the coefficients of the left-hand-side of equation (G.10), and explicitly

contained within the right-hand-side matrices [FV(k)], k=1,...4. The temperature variable is implicitly contained within the [FV(5)] matrix.

Note that the usual quasi-linearization* of the radiation term has been used in equation (G.10). However, even without the radiation term, equation (G.10) is an extremely non-linear ordinary differential equation and must be solved using some sort of iterative procedure. When the B_1 and B_2 contributions are ignored, then $a_1(T) = c_v$, $a_2(T) = a_3(T) = a_4(T) \equiv 0$ and, if there is no radiation, the left-hand-side of equation (G.10) takes the more familiar form of $\rho c_v[\dot{T}] + [KT][T]$.

Excluding the implicit time-dependency of the $a_i(T)$ coefficients, the left-hand-side of equation (G.10) can be rewritten in the following form of temperature-dependent spatial integrals times the time-dependent temperature,

$$\text{L.H.S.} \rightarrow \quad ([C0] + [C1] + [C2])\,[\dot{T}] + ([K0] + [K1] + [K2] + [K3] + [K4])\,[T], \qquad \text{(G.11)}$$

where

$$[C0] = \int_{V(j)} \rho a_1(T)\,[CT]\,dVol,$$

$$[C1] = \int_{V(j)} \rho a_2(T)\,b_1(T)\,[CT]\,dVol,$$

$$[C2] = \int_{V(j)} \rho \frac{\partial B_2}{\partial T^2}\,b_1^2(T)\,[CT]\,dVol,$$

$$[K0] = \int_{V(j)} [BT]\,[KT]\,[BT]\,dVol,$$

$$[K1] = \int_{S_b(j)} \bar{h}\,[CT]\,dS,$$

$$[K2] = \int_{S_c(j)} a(T,T_\infty)\,[CT]\,dS,$$

$$[K3] = \int_{V(j)} \rho a_3(T)\,[CT]\,dVol,$$

$$[K4] = \int_{V(j)} \rho a_4(T)\,b_1(T)\,[CT]\,dVol,$$

$$[CT] = [NTE]^T\,[NTE],$$

$$b_1(T) = [NTE]^T\,[T] = \sum_{i=1}^{NPT(j)} NTE_i T_i(t).$$

*$(T^4 - T_\infty^4) = (T^2 + T_\infty^2)\,(T + T_\infty)\,(T - T_\infty) \rightarrow a(T, T_\infty)\,(T - T_\infty)$.

AD-A165 295 A PHYSICAL MODEL AND CONSERVATION EQUATIONS FOR DYNAMIC 2/2
SOLID-LIQUID BEHAVIOR(U) VILLANOVA UNIV PA DEPT OF
MECHANICAL ENGINEERING J N MAJERUS FEB 86 BRL-CR-551
UNCLASSIFIED DAAK11-83-K-0009 F/G 20/4 NL

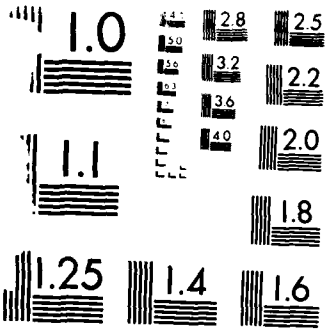

MICROCOPY RESOLUTION TEST CHART
NATIONAL BUREAU OF STANDARDS-1963 A

Note that a mild nonlinearity is introduced by the [CO] and [K3] terms, whereas, stronger nonlinearities are introduced respectively by the [C1], [K4], [C2] and [K2] terms. The volume and surface integrals cannot be numerically evaluated until the temperature is known, and hence these temperature-dependent spatial integrals can only be determined in some iterative manner.

In order to discretize equation (G.10) with respect to time, equation (G.10) is multiplied by a piecewise, non-zero, time-dependent weighting function WTE(t) and a trial function is introduced to approximate the temporal temperature behavior, i.e.,

$$WTE(t) = \sum_{m=0}^{NT} WTE_m(t), \tag{G.12}$$

and

$$[T(t)] \cong \sum_{m=0}^{NT} N_{te}\,[T(m)], \tag{G.13}$$

where $[T(m)]$ represents the TNP nodal temperatures at time t_m, and N_{te} is the time-dependent interpolation function for the temperature. Integrating over the entire time interval of interest, and using equation (G.11), the energy equation becomes the following set of nonlinear algebraic equations for each time-step,

$$\left\{\int_{t_s} \frac{2}{\Delta t_m} ([CO] + [C1] + [C2])\, WTE_m(\bar{\tau})\, [\dot{N}_{te}]\, d\bar{\tau}\right.$$

$$\left.+\int_{t_s} ([KO] + [K1] + [K2] + [K3] + [K4])\, WTE_m(\bar{\tau})\, [N_{te}]\, d\bar{\tau}\right\} \tag{G.14}$$

$$[T(m)] = \int_{t_s} \{[q] + [\dot{Q}] + [h] - [IE] + [RD] + \sum_{k=1}^{5} [FV(k)]\} WTE_m(\bar{\tau})\, d\bar{\tau},$$

where $[q] = \int_{S_a(j)} [NTE]^T q\, dS,$

$$[\dot{Q}] = \int_{V(j)} \rho [NTE]^T \dot{Q}\, dVol,$$

$$[h] = \int_{S_b(j)} \bar{h}\, T_\infty\, [NTE]^T\, dS,$$

$$[IE] = \int_{S_p(t)} [NTE]^T (\text{Internal energy})\, (\rho [N]^T [\bar{V}]\cdot n)\, dS,$$

$$[RD] = \int_{S_c(j)} [NTE]^T a(T,T_\infty)\, T_\infty dS.$$

Note that the [FV] terms include the time-dependent function $[\bar{V}] \cong [N_t(\bar{\tau})]\ [\bar{V}(n)]$, which is explicitly given by equation (F.5). Also, the time-step Δt_m for the thermal approximation could be larger than the Δt_n used in the velocity approximation, in which case the $[\bar{V}]$ term would involve a sum of interpolation terms.

If a quadratic time-element is assumed for the temperature behavior, then the algebraic equations take the form of equations (F.9) or (F.11). Similarly, the coefficients are given by Tables F-3 through F-6, with the [GXYZ] and [G] matrices omitted, all coefficients multiplied by Δt_n, and the following substitutions made: $([KE] + [KEN]) \rightarrow [\overline{KT}]$, and $[M] \rightarrow [\overline{CT}]^n$ where

$$[\overline{KT}] \equiv \int_{t_s} ([K0] + [K1] + [K2] + [K3] + [K4])\ WTE_m\ (\bar{\tau})\ [N_{te}]\ d\bar{\tau},$$

$$[\overline{CT}] \equiv \int_{t_s} ([C0] + [C1] + [C2])\ WTE_m\ (\bar{\tau})\ [\dot{N}_{te}]\ d\bar{\tau}.$$

For ballistic penetration problems, the temperature change between time-steps might be realistically modeled using a linear variation. If a single weighting function $WTE_m(\bar{\tau})$ is assumed over the time interval, then equation (G.14) becomes the classical "implicitness θ" equation ($0 \leq \theta \leq 1$) for a first order equation, i.e.,

$$\left\{\frac{1}{\Delta t_n}\ [\overline{CT}(T_{n+\theta})] + \theta\ [\overline{KT}(T_{n+\theta})]\right\} T_{n+1} + \left\{\frac{-1}{\Delta t_n}\ [\overline{CT}(T_{n+\theta})]\right. \tag{G.15}$$

$$\left. + (1-\theta)\ [KT(T_{n+\theta})]\right\} T_n = F_{n+\theta},$$

where

$$T_{n+\theta} = (1-\theta)\ T_n + \theta T_{n+1},$$

$$F_{n+\theta} = (1-\theta)\ F_n + \theta F_{n+1},$$

and which can be solved for T_{n+1} using a linear iteration.

Rather than the above linear iteration, Baker[4] uses a Newton-Raphson iteration scheme of the following form,

$$[J(H_{n+1})]^P\ [\delta T_{n+1}]^{P+1} = -\ [H_{n+1}]^P, \tag{G.16}$$

where

$$[T_{n+1}]^{P+1} = [T_{n+1}]^P + [\delta T_{n+1}]^{P+1},$$

$$[H_{n+1}]^P = \frac{[\overline{CT}_{n+\theta}]^P}{\Delta t_n}\ \{[T_{n+1}]^P - [T_n]\} + \theta\ [\overline{KT}_{n+1}]^P\ [T_{n+1}]^P + (1-\theta)$$

$$[\overline{KT}_n]\ [T_n] + \theta\ [F_{n+1}] + (1-\theta)\ [F_n],$$

$$[J(H_{n+1})]^P = \partial[H]/\partial[T],$$

$$= \frac{[\overline{CT}]}{\Delta t_n} + \theta[\overline{KT}] + \left(\frac{1}{\Delta tn}\ \frac{\partial[\overline{CT}]}{\partial[T]} + \theta\frac{\partial[\overline{KT}]}{\partial[T]}\right)[T_{n+1}]^P + \frac{\partial[F]}{\partial[T]}.$$

During the second year of this research, several first order, non-linear, equations will be evaluated using a variety of the above techniques, and several of the most promising techniques will be selected.

DISTRIBUTION LIST

No. of Copies	Organization
12	Administrator Defense Technical Info Center ATTN: DTIC-DDA Cameron Station Alexandria, VA 22304-6145
1	HQDA DAMA-ART-M Washington, DC 20310
1	Commander US Army Materiel Command ATTN: AMCDRA-ST 5001 Eisenhower Avenue Alexandria, VA 22333-0001
1	Commander Armament R&D Center US Army AMCCOM ATTN: SMCAR-TSS Dover, NJ 07801
1	Commander Armament R&D Center US Army AMCCOM ATTN: SMCAR-TDC Dover, NJ 07801
1	Director Benet Weapons Laboratory Armament R&D Center US Army AMCCOM ATTN: SMCAR-LCB-TL Watervliet, NJ 12189
1	Commander US Army Armament, Munitions and Chemical Command ATTN: SMCAR-ESP-L Rock Island, IL 61299
1	Commander US Army Aviation Research and Development Command ATTN: AMSAV-E 4300 Goodfellow Blvd. St. Louis, MO 63120
1	Director US Army Air Mobility Research and Development Laboratory Ames Research Center Moffet Field, CA 94035
1	Commander US Army Communications Electronics Command ATTN: AMSEL-ED Fort Monmouth, NJ 07703
1	Commander ERADCOM Technical Library ATTN: DELSD-L (Reports Section Fort Monmouth, NJ 07703-5301
1	Commander US Army Missile Command Research, Development and Engineering Center ATTN: AMSMI-RD Redstone Arsenal, AL 35898
1	Commander US Army Missile and Space Intelligence Center ATTN: AIAMS-YDL Redstone Arsenal, AL 35898-5500
1	Commander US Army Tank Automotive Command ATTN: AMSTA-TSL Warren, MI 48090
1	Director US Army TRADOC Systems Analysis Activity ATTN: ATAA-SL White Sands Missile Range NM 88002
1	Commandant US Army Infantry School ATTN: ATSH-CD-CSO-OR Fort Benning, GA 31905

DISTRIBUTION LIST

No. of Copies	Organization
1	Commander US Army Development & Employment Agency ATTN: MODE-TED-SAB Fort Lewis, WA 98433
1	AFWL/SUL Kirtland AFB, NM 87117
1	Air Force Armament Laboratory ATTN: AFATL/DLODL Eglin AFB, FL 32542-5000
1	Assistant Secretary of the Army (R&D) ATTN: Asst for Research Washington, DC 20310
2	Commander Armament R&D Center US Army AMCCOM ATTN: Mr. G. Randers-Pehrson Mr. J. Pearson Dover, NJ 07801
2	Commander US Army Materials and Mechanics Research Center ATTN: AMXMR-RD, J. Mescall Tech Lib Watertown, MD 02172
1	Commander US Army Research Office P.O. Box 12211 Research Triangle Park NC 27709
2	Chief of Naval Research Dept. of the Navy ATTN: Code 427 Code 470 Washington, DC 20325
1	Commander Naval Sea Systems Command ATTN: Code SEA-62R Washington, DC 20362
4	Commander Naval Surface Weapons Center ATTN: Code 730 Code DG-50 DX-21, Lib Br N. Coleburn, R-13 White Oak, MD 20910
4	Commander Naval Surface Weapons Center ATTN: Code G-10 (H. Oliver) Code G-13 (D. Dickenson) (T. Wasmund) (J. Bland) Dahlgren, VA 22448
5	Naval Weapons Center ATTN: Code 3835 (M. Backman) (J. Schulz) Code 3261 (M. Alexander) Code 3181 (J. Morrow) (C.Gillespie) China Lake, CA 93555
1	David W. Taylor, Naval Ship R&D Center ATTN: D. R. Garrison, Code 1740.3 Bethesda, MD 20084
1	Commander Naval Research Laboratory Washington, DC 20375
1	USAF/AFRDDA Washington, DC 20311
1	AFSC/SDW/SDOA Andrews AFB, MD 20334
2	Commander Naval Air Systems Command ATTN: Code AIR-310 Code AIR-350 Washington, DC 20360
1	AFAL/WR Wright-Patterson AFB, OH 45433

DISTRIBUTION LIST

No. of Copies	Organization
10	Central Intelligence Agency Office of Central Reference Dissemination Branch Room GE-47 HQS Washington, DC 20502
3	Commander AFATL ATTN: DLJR (J. Foster) DLYV (A. Rutland) DLYV (J. Gagliano) Tech Lib Eglin AFB, FL 32542
1	US Air Force Academy ATTN: Code FJS-41 (NC) Tech Lib Colorado Springs, CO 80840
6	Director Lawrence Livermore Laboratory ATTN: Dr. J. Kury Dr. M. Wilkins Dr. E. Lee Dr. H. Horning Dr. M. Van Thiel P. O. Box 808 Livermore, CA 94550
1	Battelle-Columbus Laboratories ATTN: Technical Library 505 King Avenue Columbus, OH 43201
1	Dyna East Corporation ATTN: P. C. Chou 227 Hemlock Road Wynnewood, PA 19096
1	Aerojet Ordnance Corporation ATTN: Warhead Tech. Dept. Dr. J. Carleone 2521 Michelle Drive Tustin, CA 92680
1	Physics International Company Tactical Systems Group Eastern Division ATTN: E. R. Berus 901 Seville Road Wadsworth, OH 44281
1	S-CUBED ATTN: Dr. R. Sedgewick P. O. Box 1620 La Jolla, CA 92038-1620
1	Physics International Company Ordnance Technology Dept. Computational Physics Group ATTN: D. Davidson 2700 Merced Street San Leandro, CA 94577
4	University of California Los Alamos Scientific Lab ATTN: Dr. J. Walsh Dr. R. Karpp, M4, MS940 Dr. C. Mautz Technical Library P. O. Box 1663 Los Alamos, NM 87545
1	University of Denver Denver Research Institute ATTN: Mr. R. F. Recht 2390 S. University Blvd. Denver, CO 80210
2	University of Illinois Dept. of Aeronautical and Astronautical Engineering ATTN: Prof. A. R. Zak Prof. S. M. Yen Urbana, IL 61801
2	Honeywell, Inc. Government and Aerospace Products Division 600 Second St. NE ATTN: J. Blackburn T. Helvig Hopkins, NM 55343

DISTRIBUTION LIST

No. of Copies	Organization
1	Sandia Laboratories ATTN: Tech Lib Albuquerque, NM 87115
1	Southwest Research Institute Division of Eng. & Mat'l Sci. ATTN: Dr. C. E. Anderson, Jr. 8500 Culebra Road San Antonio, TX 78228
1	Michigan Technological University Dept of ME & EM ATTN: Prof. W. Predebon Houghton, MI 49931
1	Falcon R & D Company ATTN: R. K. Miller 109 Inverness Dr. East Englewood, CO 80112
1	California Research and Technology ATTN: Mr. Mark Majerus Suite B130 11875 Dublin Blvd. Dublin, CA 94568
2	Dr. J. N. Majerus Mechanical Engr Dept. Tolentine Hall Villanova University Villanova, PA 19085

Aberdeen Proving Ground

Dir, USAMSAA
ATTN: AMXSY-D
AMXSY-MP, H. Cohen
AMXSY-R, R. Simmons

Cdr, USATECOM
ATTN: AMSTE-TO-F

Cdr, CRDC, AMCCOM
ATTN: SMCCR-RSP-A
SMCCR-MU
SMCCR-SPS-IL

USER EVALUATION SHEET/CHANGE OF ADDRESS

This Laboratory undertakes a continuing effort to improve the quality of the reports it publishes. Your comments/answers to the items/questions below will aid us in our efforts.

1. BRL Report Number_____ Date of Report_____

2. Date Report Received_____

3. Does this report satisfy a need? (Comment on purpose, related project, or other area of interest for which the report will be used.)_____

4. How specifically, is the report being used? (Information source, design data, procedure, source of ideas, etc.)_____

5. Has the information in this report led to any quantitative savings as far as man-hours or dollars saved, operating costs avoided or efficiencies achieved, etc? If so, please elaborate._____

6. General Comments. What do you think should be changed to improve future reports? (Indicate changes to organization, technical content, format, etc.)

CURRENT ADDRESS

Name

Organization

Address

City, State, Zip

7. If indicating a Change of Address or Address Correction, please provide the New or Correct Address in Block 6 above and the Old or Incorrect address below.

OLD ADDRESS

Name

Organization

Address

City, State, Zip

(Remove this sheet along the perforation, fold as indicated, staple or tape closed, and mail.)

FOLD HERE

Director
U.S. Army Ballistic Research Laboratory
ATTN: SLCBR-DD-T
Aberdeen Proving Ground, MD 21005-5066

NO POSTAGE
NECESSARY
IF MAILED
IN THE
UNITED STATES

OFFICIAL BUSINESS
PENALTY FOR PRIVATE USE, $300

BUSINESS REPLY MAIL
FIRST CLASS PERMIT NO 12062 WASHINGTON, DC
POSTAGE WILL BE PAID BY DEPARTMENT OF THE ARMY

Director
U.S. Army Ballistic Research Laboratory
ATTN: SLCBR-DD-T
Aberdeen Proving Ground, MD 21005-9989

FOLD HERE

END

DTIC

FILMED

4-86